IDO-14574

CHEMICAL PROCESSING TECHNOLOGY QUARTERLY PROGRESS REPORT

July – September, 1961

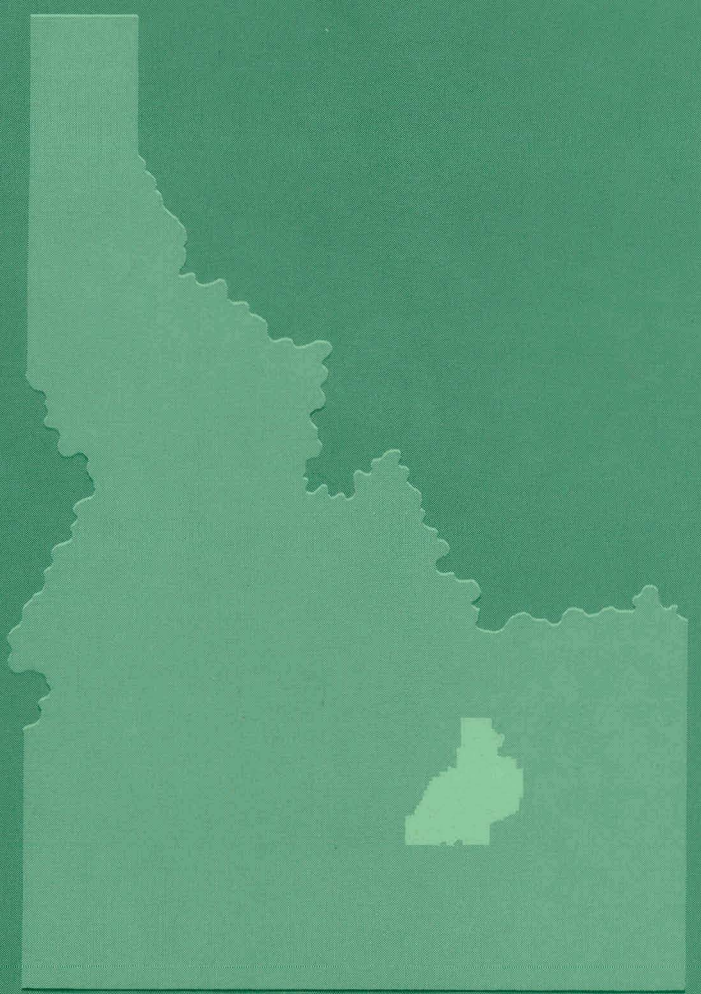

PHILLIPS PETROLEUM COMPANY

PHILLIPS 66

ATOMIC ENERGY DIVISION

NATIONAL REACTOR TESTING STATION

US ATOMIC ENERGY COMMISSION

DISCLAIMER

PRICE $1.25

Available from the
Office of Technical Services
U. S. Department of Commerce
Washington 25, D. C.

LEGAL NOTICE

This report was prepared as an account of Government sponsored work. Neither the United States, nor the Commission, nor any person acting on behalf of the Commission:

A. Makes any warranty or representation, express or implied, with respect to the accuracy, completeness, or usefulness of the information contained in this report, or that the use of any information, apparatus, method, or process disclosed in this report may not infringe privately owned rights; or

B. Assumes any liabilities with respect to the use of, or for damages resulting from the use of any information, apparatus, method, or process disclosed in this report.

As used in the above, "person acting on behalf of the Commission" includes any employee or contractor of the Commission, or employee of such contractor, to the extent that such employee or contractor of the Commission, or employee of such contractor prepares, disseminates, or provides access to, any information pursuant to his employment or contract with the Commission, or his employment with such contractor.

Printed in USA

ERRATA

IDO-14574

CHEMICAL PROCESSING TECHNOLOGY QUARTERLY PROGRESS REPORT
July - September, 1961

1. The first compound in line 3 on page 15 should be: $Al(NO_3)_3$.

2. The constants K_1, S_1, and S_2 in line 16 on page 21 are in error. They should read as follows:

K_1	0.221
S_1	0.0021
S_2	0.00040

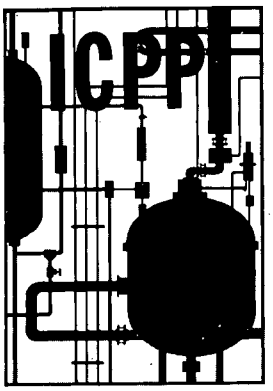

IDAHO CHEMICAL PROCESSING PLANT

IDO-14574
AEC Research & Development Report
General, Miscellaneous, and Progress Reports
TID-4500 (16th Ed.)
Issued: December 18, 1961

CHEMICAL PROCESSING TECHNOLOGY QUARTERLY PROGRESS REPORT

JULY - SEPTEMBER, 1961

J. R. Huffman
Assistant Manager, Technical

J. A. McBride
Technical Director

J. R. Bower
Editor

PHILLIPS
PETROLEUM
COMPANY

Atomic Energy Division
Contract AT(10-1)-205
Idaho Operations Office
U. S. ATOMIC ENERGY COMMISSION

Previous Quarterly Reports in the ICPP Series

1954

Quarter	Number
2	IDO-14324
3	IDO-14337
4	IDO-14350

1955

Quarter	Number
1	IDO-14354
2	IDO-14362
3	IDO-14364
4	IDO-14383

1956

Quarter	Number
1	IDO-14385
2	IDO-14391
3	IDO-14395
4	IDO-14400

1957

Quarter	Number
1	IDO-14410
2	IDO-14419
3	IDO-14422
4	IDO-14430

1958

Quarter	Number
1	IDO-14443
2	IDO-14453
3	IDO-14457
4	IDO-14467

1959

Quarter	Number
1	IDO-14471
2	IDO-14494
3	IDO-14509
4	IDO-14512

1960

Quarter	Number
1	IDO-14520
2	IDO-14534
3	IDO-14540
4	IDO-14553

1961

Quarter	Number
1	IDO-14560
2	IDO-14567

CHEMICAL PROCESSING TECHNOLOGY
QUARTERLY PROGRESS REPORT
JULY - SEPTEMBER, 1961

SUMMARY

The Idaho Chemical Processing Plant did not operate on fuel recovery during this period since numerous repairs and modifications were being made to the extraction and uranium concentration equipment. Barium-140 production continued on schedule; substantial decontamination of the RaLa facility was achieved and desirable replacement or repair of in-cell equipment was accomplished in the interval between two successive runs.

Aqueous zirconium fuel processing studies have continued with the objective of adapting the hydrofluoric acid process to continuous dissolution and complexing in order to increase the capacity of the ICPP process while using as much existing equipment as possible to minimize costs. Dissolution rates for Zircaloy-2 in 10M fluoride dissolver solution proved to be adequate for continuous dissolution (as high as 79 mg cm^{-2} min^{-1}) in an acid range which resulted in both controlled gas evolution and stable dissolver solutions. Preliminary results indicate the possibility of blending zirconium raffinates from this process with larger volumes of aluminum raffinates to achieve stable waste solutions and avoid the necessity of constructing additional special alloy tanks for zirconium waste. Supplemental studies on the sodium formate process for head end precipitation of zirconium and fluoride are reported, as well as results of corrosion tests on materials of construction considered for use in various zirconium processing applications.

Other aqueous processing studies included the determination that 2.2M aluminum nitrate solutions, acid deficient to 1.0N^b, could be used to scrub highly acid uranium extraction solutions without incurring the hazard of ammonium diuranate precipitation. Preliminary to processing organic moderated reactor fuel elements, it was discovered that carbonaceous films present on some elements were resistant to removal by Turco 4502 solution, and responded only to oxidation at 500°C; the possibility of processing without film removal was explored with satisfactory results insofar as dissolution of the fuel is concerned.

Electrolytic dissolution of nichrome-containing fuels in nitric acid appears promising and conditions predicted from earlier studies on stainless-steel dissolution were confirmed. Stability, density, and viscosity data are presented for representative product solutions from electrolytic dissolution of stainless-steel fuel of the APPR type. Results of additional chemical and radiation exposure tests on possible plastic insulator materials are presented.

Factors affecting the formation of alpha alumina from amorphous alumina received additional study in the laboratory because of the severe attrition problem and related operational difficulties associated with the alpha form in the fluidized-bed calcination process. It was demonstrated that very little

alpha alumina was formed by heating amorphous pilot plant product in air, moderate amounts were formed by heating in an air-water vapor atmosphere, and larger amounts were formed when the atmosphere also contained nitric acid vapors. Temperature and method of alumina formation (ie, conditions of pilot plant calciner operation) also affected the conversion but appeared to be interrelated so that no clear cut conclusion on individual effects could be drawn. Investigations of intermediates in the reaction, and structure and distribution of crystalline material in individual particles of calcine, are discussed.

Pilot plant calcination studies showed a direct effect between feed sodium content and alpha alumina formation rate. Mercury was found to have no detectable effect on the process or product.

Stripping of TBP from aqueous uranium streams was investigated because of difficulty associated with decomposition products of TBP, which form gummy deposits and interfere with the operation of product evaporators and pumps. Using tracer phosphorus, the TBP distribution coefficient between Amsco and water containing flowsheet quantities of nitric acid and uranium was found to be sufficiently high (290 $\pm$ 31) that stripping with Amsco should have presented no problem. However, an inextractable phosphorus species was detected. This species formed under the influence of hydrolysis, radiolysis, or both, and limited phosphorus removal to a TBP equivalent of 1×10^{-3} g/l.

Other basic process studies reported include analog simulation of air pulsers, dynamics of a new thermosiphon evaporator, and background information on extraction column kinetics.

CHEMICAL PROCESSING TECHNOLOGY
QUARTERLY PROGRESS REPORT
JULY - SEPTEMBER, 1961

CONTENTS

FIGURES

TABLES

I. ICPP OPERATIONAL SCHEDULE, PERFORMANCE, AND PROBLEMS

1. ICPP PROCESSING SCHEDULE
(J. R. Bower)

The Idaho Chemical Processing Plant did not operate on fuel recovery during this period since numerous repairs and modifications were being made to the extraction and uranium concentration equipment. A discussion of the principal changes was presented in an earlier quarterly report [1]*. These include replacement of remote diaphragm pulse units with direct air pulsers on all extraction and stripping columns, replacement of diaphragm pumps with air lifts on in-cell process streams, and modification of product evaporators to minimize criticality hazards. In addition, glass Raschig rings with a boron content >12 percent were placed on the floor of the first cycle product storage cell to protect against the possible nuclear hazard in case of equipment leakage. This will permit storage of larger volumes of more concentrated uranium solutions. Gravity cell floor drains were permanently blocked and transfer jets installed in the sumps to prevent possible escape of uranium solutions through leaking floor drain valves.

The Demonstrational Waste Calcining Facility was operated for a short time at the end of this period. A discussion of findings is included in Section V of this report since developmental rather than production aspects are of prime concern at the present stage of operation.

Four barium-140 runs were completed, yielding batches of 21,600 to 26,900 curies of product (45 to 53 percent of theory.) The cell was decontaminated during this period in order to make repairs which had become advisable, although the process was still operable through use of alternate equipment. Decontamination was accomplished in 12 days to radiation levels sufficiently low to make the necessary repairs and replacements.

Initial decontamination procedures consisted of alternate flushes of 10 percent HNO_3 and 10 percent NaOH containing 2.5 percent tartaric acid. Steaming of certain vessels was started after the first three flushes were completed. As the decontamination proceeded, rinses of Turco 4306-C, NaF - $Al(NO_3)_3$, and oxalic acid were utilized. Decontamination of exterior surfaces was started after eight acid and six caustic flushes had been completed.

The first radiation measurements were taken after two acid flushes had been routed through the equipment. A Jordan head on an extension cord was lowered into the cell through the elevator opening. A reading of 35 r/hr was encountered at the top of the cell and it increased as the head was lowered until a reading of > 500 r/hr was obtained in the centrifuge area. Twelve days after starting the decontamination, the radiation readings were reduced to a general field in the mr range with 5-r/hr spots throughout the cell. These levels permitted working times of 8 to 25 minutes for a one-week exposure.

---

* Numbers in brackets refer to entries in Section VIII, References.

The major in-cell work completed during this shutdown consisted of installation of a new elevator cable, new brushes on the centrifuge motor, and new heater elements and leads in the product drier. Many minor jobs such as lubricating the manipulator and positioner, replacing cell lights, cleaning and tightening the viewing window, and checking oil line unions also were completed.

2. PLANT CORROSION STUDIES
(N. D. Stolica, Problem Leader; T. L. Hoffman)

2.1 Corrosion in the CPP Storage Basin

A visual examination of equipment, which is positioned underwater in the CPP fuel storage basin, indicated that corrosion had taken place on the galvanized hanger yokes and the aluminum rack in the underwater saw facility. A chemical analysis of the basin water gave the following composition: nitrate 263 ppm, sodium 117 ppm, chloride 50.8 ppm, chlorine 0.15 ppm, and pH 7.8. These concentrations of the chemical constituents in the basin water were not considered unduly corrosive.

The underwater parts of the galvanized steel hanger yokes were uniformly covered with rust. However, this equipment had been in service for approximately ten years, and the amount of corrosion was considered about normal for this type of material in such service. It was recommended that the yokes be replaced or regalvanized.

The aluminum corrosion product was amorphous to X-ray diffraction, and a qualitative spectrographic analysis indicated aluminum and silicon as major constituents, with iron and sodium as minor constituents. The silicon probably came from the diatomaceous earth filters in the basin. The aluminum probably was present as amorphous hydrated aluminum oxide. Additional studies are planned to determine the reasons for the corrosion of the aluminum racks.

2.2 Corrosion in Product Evaporator Service

A service test corrosion evaluation was conducted on the heat exchanger tube bundle and on the deentraining head of a continuous thermosiphon evaporator which had been replaced after about 14,000 hr service as an intercycle uranium product evaporator (Vessel H 110). This evaporator was constructed of type 348 seamless stainless steel.

An unaided eye examination showed that all the tubes within the steam chest were free of perforations, pits or areas of localized corrosive attack. However, severe end grain attack occurred at the feed end of the tubes at the lower tube sheet. A micro examination of specimens and photos of the upper tube sheet-tube welds indicated that the cross sectional thickness of the weld deposit was less than the tube thickness and that interdendritic attack had occurred on the weld deposit. In addition a ductile fracture had occurred in the weld deposit. No evidence of corrosion was found in the vapor head pipe section, the inlet, or the outlet.

II. AQUEOUS PROCESS STUDIES

(Section Chief: K. L. Rohde, Chemistry;
Group Leaders: D. W. Rhodes, R. D. Fletcher)

Because of the ICPP role as an AEC reprocessing facility for highly enriched uranium fuels incorporating aluminum, zirconium and stainless steel, major technical functions include maintenance and improvement of these processes as well as development of processes for new or improved fuel types.

A process improvement of major interest at the present time is the increase in capacity of the original head end process for zirconium alloy fuels of the PWR-seed type from the existing one kg/day of uranium to 5 to 10 kg/day. The most promising way of achieving this appears to be by the use of continuous hydrofluoric acid dissolution of the fuel followed by continuous complexing with aluminum nitrate. Results are reported on the rate of dissolution of Zircaloy-2 in hydrofluoric acid-zirconium fluoride solutions; these data will be used in the development of the continuous dissolution flowsheet. Results of preliminary studies on stability (ie, resistance to precipitation) of blended raffinates from the zirconium and aluminum processes are given. Corrosion studies will be made on these same blended raffinates. The extent of liquid and vapor corrosion of Monel in dissolver vessel application is reported for hydrofluoric acid dissolution in the presence of hydrogen peroxide.

Advanced and significantly improved processes for zirconium-uranium alloys also have been under development at the ICPP. One approach has been to separate the major component, zirconium, from the majority of fission products and the uranium in a head end operation following dissolution; the solids would be stored in low-cost underground containers. Either of two precipitation processes looks promising for the removal of zirconium from solutions obtained from hydrofluoric acid dissolution of Zircaloy-2 uranium fuel. One is the precipitation of barium fluozirconate and the other is the precipitation of zirconium fluoride by sodium formate. Process modifications are described for the latter process in which solid sodium formate is added as the precipitant instead of sodium formate from an aqueous solution.

Aluminum process developments include results of a study of pH of 2.2M aluminum nitrate solutions as acid deficiency was increased to 1.0N[b]. The maximum pH observed was below that at which precipitation of uranium is known to be a problem, thus indicating the possibility of using greater acid deficiency in scrub solutions to treat high acid concentrations in feed solutions.

During previous studies on the Diban process for dissolving uranium-aluminum alloy fuels, considerable data on the physical properties of the system were obtained. An equation is reported relating the density to the composition of solutions of aluminum nitrate of varying basicity.

OMRE fuel contains an adherent layer of carbonaceous residue when it is discharged from the reactor. The residue on the first core from OMRE was readily removed at the ICPP by Turco 4502 prior to reprocessing. In preparing to reprocess the second core from OMRE, current experiments in the ICPP multicurie cell have shown that Turco 4502 produced only partial removal of the carbonaceous film from test specimens. Removal was accomplished only by heating for two hr at 500°C in air. Scoping studies showed

that the uncleaned fuel pieces would dissolve readily in hot 6M sulfuric acid or electrolytically in nitric acid. Either dissolver solution gave low disengaging times with 10 percent TBP in Amsco in the emulsion tester in spite of the presence of undissolved carbon. Further work is needed to establish the feasibility of integrally dissolving uncleaned OMRE fuel and processing it, by solvent extraction, in the plant. Attempts were made to clean pyrolytically-fouled samples from Phillips Petroleum Co's EOCR program, from the California Research Corp., and from Atomics International.

Six slugs of irradiated thorium clad in aluminum were dissolved in the Hot Cell as assistance to the fuel development program at MTR Technical. The batch dissolutions required contact for 26 to 30 hr in 15M nitric acid-0.04M hydrofluoric acid at the boiling point.

1. AQUEOUS ZIRCONIUM FUEL PROCESSING

1.1 Dissolution Kinetics in Hydrofluoric Acid (J. W. Codding, Problem Leader; B. E. Paige)

Continuous dissolution of Zircaloy-2-clad, zirconium-uranium alloy fuel is being studied at the ICPP for possible use on zirconium fuels containing up to 3.0 percent uranium. Dissolution rates of Zircaloy-2 fuel pieces were measured by incremental batch dissolution in dissolver product solutions of various compositions. Dissolver product concentration was used because it corresponds to the composition of a stirred-tank type of continuous dissolver. Nitric acid or aluminum nitrate were used as uranium oxidants in two experiments.

1.11 Methods and Equipment. The batch dissolution experiments were conducted at 95 to 97°C in 800-ml Teflon beakers, fitted with polyethylene condensers. The voluminous hydrogen evolved during the dissolution provided adequate stirring. The surface area of the 3.5- x 1.3- x 0.5-cm coupons was calculated from vernier caliper measurements. The coupons were suspended in the dissolver product solution by means of a Teflon string for one to three min, depending on the dissolution rate.

Dissolver product solution was prepared by dissolving Zircaloy-clad fuel pieces in hydrofluoric acid with hydrogen peroxide as the oxidant. This solution was mixed with hydrofluoric acid, concentrated nitric acid, or aluminum nitrate solution to produce the desired dissolver product composition for the rate measurements.

Measurements are reported only for 10M fluoride concentration. Each reported value represents three measurements on each of two coupons. The mean value of these six measurements for each rate experiment is reported in Table I with the variance calculated for the 95 percent confidence level. Zirconium and hydrogen ion concentrations reported are the median values obtained from analysis of samples taken during the run.

1.12 Experimental Results. The experimental results for seven different sets of conditions are shown in Table I.

TABLE I

DISSOLUTION RATES OF ZIRCALOY-2 FUEL PIECES IN VARIOUS DISSOLVER PRODUCT SOLUTIONS

Composition of Solution			Mole Ratio	Other [a]	Dissolution Rate
Fluoride M	Hydrogen Ion M	Zirconium M	F/Zr	M	mg $cm^{-2}min^{-1}$
10.2	1.13	2.27	4.5		4.4 ± 0.4
10.2	1.77	2.12	4.8		18.6 ± 1.9
10.2	1.77	2.02	5.0	0.1 $Al(NO_3)_3$	14.0 ± 2.2
10.2	2.37	1.97	5.2		31.1 ± 2.8
10.2	2.40	1.97	5.2	0.3 HNO_3	28.6 ± 1.3
10.5	2.78	1.93	5.4		37.2 ± 1.8
10.2	4.26	1.67	6.1		79.2 ± 2.8

(a) < 0.005M H_2O_2 remains from preparation of dissolvent.

An increase in the dissolution rate appears to be related to either an increase in the hydrogen ion concentration or fluoride-to-zirconium ratio. Nitric acid had little effect on the dissolution rate while aluminum nitrate in the system had a slight depressing effect. Concentrations of hydrogen ion above those listed in Table I (lower zirconium concentrations) resulted in such violent gas evolution that reliable dissolution rates could not be determined with the present laboratory apparatus. Hydrogen ion concentrations below those listed in Table I (higher zirconium concentration) resulted in solutions which were unstable and precipitated solids.

Dissolution rates of Zircaloy-2 were checked in hydrofluoric acid solutions free from zirconium. The rate constant obtained at 96 ± 1°C in the range 0.3 to 1.0M hydrofluoric acid was 61.2 mg $cm^{-2}min^{-1}$/mole HF $liter^{-1}$. This compares favorably with an initial rate of 66 mg $cm^{-2}min^{-1}$/mole HF $liter^{-1}$ obtained by a different technique [2] for the dissolution of Zircaloy-2 in a hydrofluoric acid-13M nitric acid mixture.

In general, dissolution rates for Zircaloy-2 in dissolver product solution appear to be adequate for continuous dissolution. Careful control of the process variables will prevent the precipitation of solids or excessive gas evolution, either of which might be detrimental to the dissolution process.

1.2 Blending Raffinates from Zirconium and Aluminum Processes (J. W. Codding, Problem Leader; B. J. Newby)

Blending of zirconium, aluminum, and stainless-steel alloy fuel raffinates for storage in stainless-steel tanks at the ICPP has been considered at various

times in the past [3]. In response to current interest in the blending of aluminum and zirconium raffinates to reduce corrosion and make additional tank space available for the storage of zirconium raffinates, three simulated zirconium fluoride raffinates (see pages 37-39, IDO 14522 [4]) having different zirconium and aluminum concentrations were blended in various proportions with three aluminum nitrate raffinates having different aluminum concentrations. Portions of the resulting solutions were stored at 35 and 55°C; 35°C is the desired storage temperature to minimize corrosion while 55°C represents the maximum storage temperature allowed at the ICPP. The stored solutions were examined periodically to see if solids had formed.

Table II gives the compositions of the various raffinate solutions used in making the blends for the stability tests. The variation of zirconium concentration in the simulated zirconium fluoride raffinates and the variation of aluminum concentration in the aluminum nitrate raffinates should bracket

TABLE II

COMPOSITION OF RAFFINATE SOLUTIONS USED IN BLENDING STABILITY TESTS

	Zirconium Raffinate Compositions					
Type (a)	Zr M	Al M	H^+ M	F^- M	$CrO_3^=$ M	NO_3^- M
A	0.76	0.56	1.3	3.9	–	2.1
B	0.61	0.64	0.84	3.34	0.015	1.86
C	0.48	0.62	0.99	2.96	0.015	1.81

	Aluminum Raffinate Compositions			
Type (b)	Al M	H^+ M	Hg^{++} g/l	Na^+ M
D	1.75	1.0	4	0.1
E	1.62	1.0	4	0.1
F	1.50	1.0	4	0.1

(a) Zirconium raffinate A represents first cycle aqueous extraction waste from a 10M HF - 0.06M H_2O_2 flowsheet.

Raffinate B represents waste, after jet dilution, from recent ICPP production.

Raffinate C represents waste from fuel dissolution produced by the current ICPP flowsheet.

(b) Maximum and minimum aluminum values represent the extremes existing in stored ICPP aluminum raffinate wastes.

the concentrations of these ions in raffinates that are currently being produced at the ICPP or might be produced in the future. Aqueous first cycle waste tank temperatures at the ICPP vary from 26 to 55°C but engineering calculations have shown that the temperature can be kept below 35°C.

Figure 1 shows the stability of various blends after one month of storage at 35 and 55°C. In general, these preliminary stability observations indicate that a stable blend probably will consist of a high proportion of aluminum raffinate.

Past experience [4] and observations during this investigation indicate that equilibrium is reached very slowly, especially at the lower temperatures. For this reason the current study will be continued for several months. In addition, efforts will be made to determine the mechanism of the precipitation, the equilibrium composition of the solutions, and the identity of the solids. In the meantime, corrosion tests will be initiated to determine corrosion rates of type 304L stainless steel in the solutions which exhibit potential long-term stability.

1.3 Corrosion of Monel in Hydrofluoric Acid-Hydrogen Peroxide Mixtures (N. D. Stolica, Problem Leader; T. L. Hoffman)

The corrosion of Monel has been measured in a series of batch dissolutions of zirconium-uranium alloy fuel in hydrofluoric acid-hydrogen peroxide.

Although Monel corrosion rates of about 20 mil/month had been determined during the development of the Perflex Process at ORNL, [5] it had been shown at ICPP [4] that a practical batch dissolution flowsheet could be evolved for the alloy fuels containing greater than two percent uranium by the addition of hydrogen peroxide. Therefore, it was important to establish more exactly the behavior of Monel during dissolutions on a specific plant flowsheet to determine whether the existing plant dissolver could be used for fuel which would require a strong oxidant for homogeneous dissolution.

1.31 Experimental Methods and Materials. In addition to several preliminary studies, which are summarized below, the main test involved exposure of welded and unwelded Monel coupons to liquid and vapor during 50 batch dissolutions in the laboratory. The dissolutions were made following the flowsheet of Table III. The operation is divided into three parts. One hr was allowed for Zircaloy-2 cladding dissolution in pure hydrofluoric acid. This was followed by a 1-1/2-hr period for dissolution of the uranium-zirconium alloy in hydrofluoric acid-hydrogen peroxide, and the process was completed by a 1-hr digestion period. The reagents were metered in slowly during the first two periods to permit control of the off-gas evolution rate.

The fuel assemblies used for the dissolution were zirconium-uranium alloy clad with Zircaloy-2. The uranium content of the fuel was 2.28 to 2.44 percent. Four different plates of a fuel assembly were cut into small coupons of 30.0 to 34.0 g each, and one coupon was used for each dissolution.

The corrosion specimen alloys were factory cold-rolled and annealed wrought Monel (65.5 percent Ni, 31.7 percent Cu, 1.5 percent Fe) and Monel 60X weld wire. Each specimen (1 in. x 1 in. x 1/8 in.) was machined to a tolerance of 100 microinches root mean square (RMS) along the four edges and 500 microinches RMS on the two large surfaces. All coupons thus had

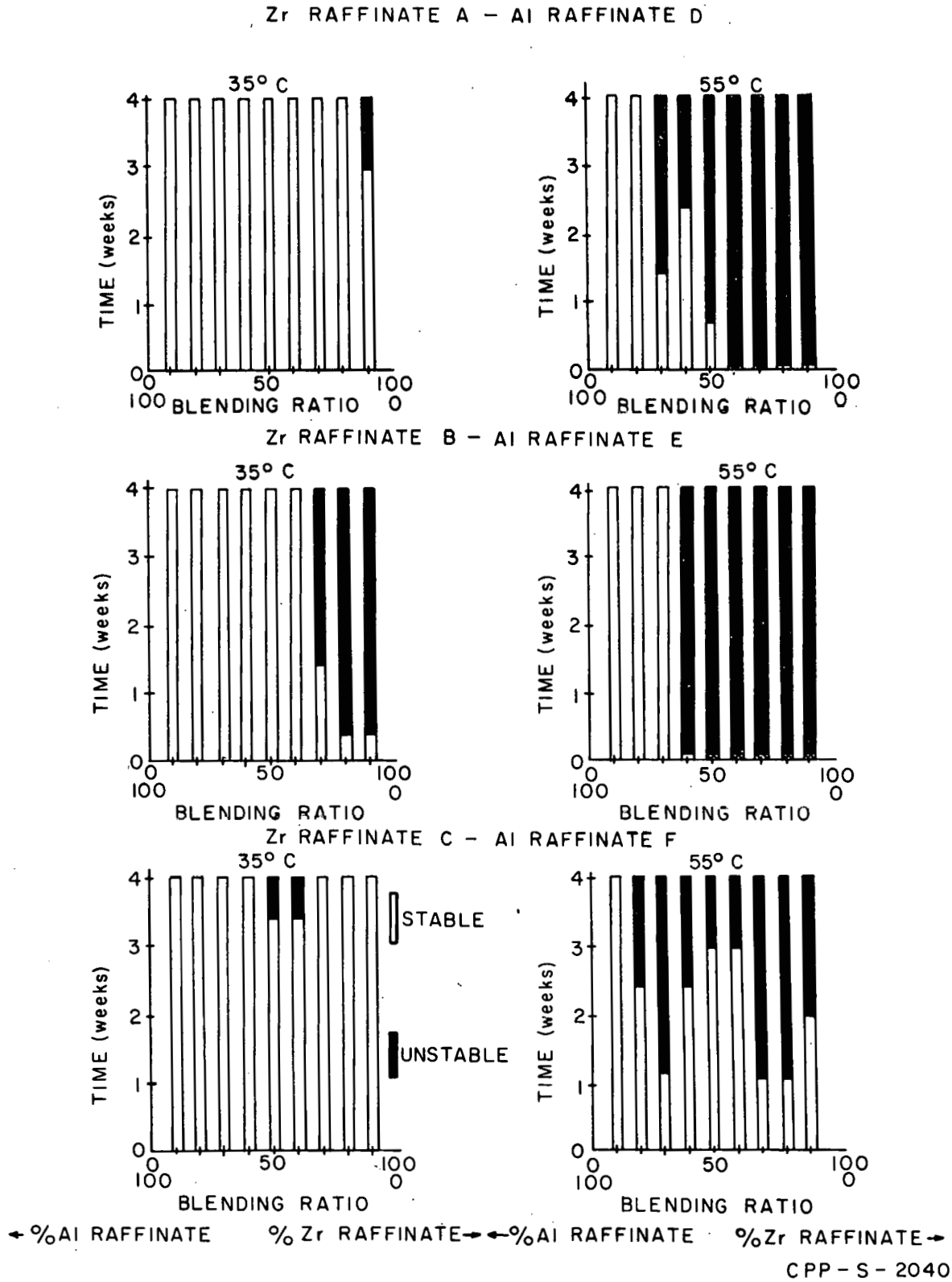

Fig. 1 Stability of zirconium fuel - aluminum fuel raffinate blends.

TABLE III

BATCH DISSOLUTION FLOWSHEET FOR ZIRCONIUM FUEL

	Fuel Charge (Wt basis) (g)	Initial Water Charge	Clad Dissolution Reagent	Alloy Dissolution Reagent	Dissolver Product
Reagent Volume, ml		50	73	73	195
Zirconium, M	(32.8)				1.85
Tin, M	(0.34)				0.15
Uranium, M	(0.83)				0.18
Fluoride, M			14.2	14.2	10.6
Acid, M			14.2	14.2	3.2
Hydrogen Peroxide, M				0.24	0.09(a)

(a) Calculated terminal peroxide concentration. Actual analysis at this point gave < 0.005M H_2O_2.

stress risers resulting from the machining operation; the welded coupons also had welding stresses.

Two welded and two unwelded Monel coupons were placed on the bottom of the Teflon dissolver (500-ml beaker plus a condenser) and similar sets of coupons were mounted on a Monel 60X wire jig and suspended 2-1/2 in. above the dissolver solution in the hot vapor.

The fuel coupons were first placed in the Teflon dissolver containing boiling water. Next, hydrofluoric acid was added continuously until one-half the required amount had been introduced in one hr. Then the mixture of hydrogen peroxide and hydrofluoric acid was added to complete the dissolution. Finally, the dissolver product was refluxed at boiling temperature for one hr. A nitrogen purge of the vapor space was used. The ratio of the terminal volume of dissolver solution to exposed surface area of the coupons was 20 ml/sq in.

The Monel specimens were cleaned, dried and weighed at the end of 35, 70, 140, and 175 cumulative hr. In addition, microscopic examinations of each specimen were made, and the final tensile strength of the Monel 60X wire jig was measured.

1.32 Experimental Results. A group of preliminary experiments indicated that 0.06M peroxide was inadequate to complete the oxidation of the uranium and that 0.25M was more than necessary. In the tests reported below, 0.09M was found to be acceptable. A series of tests with 0.25M peroxide in a flowsheet

similar to the one in Table III gave liquid and vapor phase corrosion rates of 20 and 15 mil/month, respectively. Inadequate nitrogen purging was shown to lead to higher rates in the vapor phase.

The cumulative corrosion rates of Monel during the principal batch dissolution tests are shown in Table IV. Generally, the corrosion was greater in the liquid than in the vapor phase. No effect of heat treatment of the Monel is evidenced. Interestingly, the rates for 0.09M peroxide are scarcely different from those for 0.25M. These penetration rates calculate to 0.13 mil/batch, a value similar to that obtained earlier in a very limited number of experiments [4].

Microscopic examination indicated that the Monel suffered both grain boundary and weld attack. Grain boundary attack was more severe on the samples exposed to the vapors, and knife-line attack occurred at the weld-wrought interfaces. No stress corrosion laminae were observed on the machine-finished edges of the specimens.

The embrittlement of the Monel weld wire used to support the vapor phase specimens is possibly of significance. Table V shows the tensile strengths of the Monel 60X weld wire jig that was used to support the coupons in the nitrogen-purged system. The tensile strength of a piece of unexposed Monel 60X wire is included for comparison. The data in Table V clearly show that the greatest loss of tensile strength occurred at the point where the Monel coupons were supported (2-1/2 in. above the liquid level). It is felt that this loss of strength is largely due to inadequate nitrogen purge and the elevated temperature at this location (See footnote to Table V).

These observations indicated that the use of the hydrogen peroxide batch flowsheet in the existing Monel dissolver would involve a predictably high corrosion rate. This situation might be tolerable for a limited amount of production. Standard precautions such as the use of an inert gas blanket and rinsing the dissolver free from the oxidizing agent after use are recommended.

TABLE IV

AVERAGE CUMULATIVE MONEL CORROSION RATE (MILS/MONTH) IN BOILING HYDROGEN PEROXIDE-HYDROFLUORIC ACID MIXTURES

Sample Treatment	Type Immersion	35 Hr	70 Hr	140 Hr	175 Hr [(a)]
As received	Liquid	23.9	24.2	21.7	20.0
	Vapor	8.0	7.7	5.9	6.5
As welded	Liquid	25.8	26.1	24.1	22.9
	Vapor	8.8	8.3	6.2	7.0

(a) 50 batch dissolutions

TABLE V

STRENGTH OF MONEL 60X WIRE JIG AFTER 175-HR EXPOSURE TO AIR-FREE HF-H_2O_2 VAPORS

Test Location on Specimen [a]	Tensile Strength (x1000 psi)
Part exposed 2.5 in. above liquid level [b]	89-90
Part exposed 5.0 in. above liquid level	132-133
Part exposed 9.0 in. above liquid level	135-136
Part exposed 13.0 in. above liquid level	129-130
Unexposed Monel 60X wire	156-161

(a) 3/32-in.-diameter wire.

(b) The wire located 2.5 in. above the liquid was exposed to vapors at about 100°C; wire at 5 in. or greater approached the condenser temperature of 20°C.

1.4 Zirconium Fluoride Precipitation by Sodium Formate (J. W. Codding, Problem Leader; B. J. Newby)

The addition of sodium formate to hydrofluoric acid-zirconium dissolver product solutions removes the zirconium and fluoride almost quantitatively from solution as a precipitate. Uranium losses are of the order of 0.1 percent. Adjusted supernatant solutions produced from the precipitation can be boiled down with or without the formation of solids. The boiled-down slurry or solution can be treated to form a stable extraction column feed from which uranium can be removed efficiently by extraction with 10 percent TBP in Amsco hydrocarbon.

1.41 Precipitant Concentration. Previous precipitations of zirconium and fluoride with sodium formate have been made with 3.2M solution. Addition of the precipitant as a solution more concentrated than 3.2 M would have the desirable effect of decreasing the process stream volumes. Accordingly, precipitations were made using solid sodium formate and an 8.0M sodium formate solution as the precipitants. The use of solid sodium formate produced a solid so immobile that it was difficult to stir. Larger volumes of wash solution were required to remove uranium from the precipitates formed with 8.0M sodium formate than from precipitates formed with 3.2M precipitant under identical conditions. The increased wash solution volumes offset the volume decreases realized by the use of 8.0M sodium formate solutions. In addition, the slurries formed by the use of 8.0M precipitant were too thick for easy handling.

1.42 Wash Solution Studies on Solids Formed During Boildown. Experimental work to determine the smallest volume of 0.1M nitric acid or sodium nitrate wash solution required to remove uranium from the solids formed during boildown of the supernatant liquid indicated that, at the end of three washes, the uranium in a specially-prepared sample of such solids had decreased

to 0.03 and 0.1 percent of the total uranium when 0.1M nitric acid or sodium nitrate were used, respectively. The washing approached the limit of effectiveness in three washes, as indicated by equilibrium curves. Zirconium losses of 0.1 and 0.4 percent to the wash solution (due to the solubility of the solid) occurred when the solids were washed three times with 2 ml of 0.1M sodium nitrate or nitric acid, respectively. Tenth molar acid is the more effective wash solution in removing uranium from the solids. Since the used wash solution can be kept separate from the filtrate and added to successive combined filtrates and wash solutions prior to boil-down, the greater solubility of zirconium in the nitric acid is not of prime importance.

1.43 Corrosion During Boildown. The corrosion resistance of unwelded coupons of type 316 stainless steel (extra low carbon), Carpenter-20, and Hastelloy F were tested during boil-down of the supernatant liquid and wash solutions resulting from the sodium formate precipitation. Evaporations were continued for approximately 48 hr; corrosion coupons were immersed in the liquid and also suspended above the liquid. The results are shown in Table VI. Coupons subject to system A showed negligible corrosion, while coupons subjected to system B indicated mild corrosion in the vapor and corrosion rates within the liquid varying from 2.8 to 4.2 mil/month. These studies

TABLE VI

CORROSION DURING BOILDOWN OF FILTRATE AND WASH SOLUTIONS FORMED FROM THE PRECIPITATION OF ZIRCONIUM AND FLUORIDE WITH 3.2M SODIUM FORMATE

Construction Material (unwelded)	Boildown Description	Length of Boildown (hr)	Corrosion Rate (mil /mo)	
			Liquid	Vapor
Stainless Steel 316 (ELC)	A	53	<0.04	<0.04
Stainless Steel 316 (ELC)	B	48.5	4.2	0.53
Hastelloy F	A	48	<0.04	<0.04
Hastelloy F	B	48.5	3.5	0.43
Carpenter-20	A	44	<0.04	<0.04
Carpenter-20	B	48.5	2.8	0.76

A. 240 ml of filtrate (prepared by adding 150 ml of 3.2M sodium formate at 60°C to 150 ml of dissolver solution, 0.03M in CrO_3) plus 300 ml of 0.1M $NaNO_3$ used to wash the precipitate, plus 13.8 ml of 15.7M HNO_3, boiled down to 48 ml.

B. 258 ml of filtrate (prepared by adding 150 ml of 3.2M sodium formate at 60°C to 150 ml of dissolver solution, containing 0.03M CrO_3 and 18 ml of 0.1 percent Jaguar) plus 300 ml of 0.1M HNO_3 used to wash the precipitate, plus 34.2 ml of 15.7M HNO_3, boiled down to 48 ml.

completed the preliminary work planned for the sodium formate process development. A topical report giving the complete details of the chemical work is being prepared.

2. AQUEOUS ALUMINUM FUEL PROCESSING

2.1 Acid Deficiency vs pH of 2.2M Aluminum Nitrate (D. W. Rhodes, Problem Leader; B. J. Newby)

Currently there is an interest in the use of higher ($>0.2\underline{N}^b$) acid deficiency scrub solutions for processing aluminum fuels since higher feed acidities can be tolerated in a compound column. The pH values corresponding to aluminum nitrate acid deficiencies above $0.2\underline{N}^b$ were not known, but it was known that uranium precipitates from solutions at pH 2.7 [6]. Consequently, laboratory experiments were undertaken to determine pH values corresponding to aluminum nitrate acid deficiencies over the range 0.5 to $1.0\underline{N}^b$. Since solutions of 2.2M aluminum nitrate are common at the ICPP, pH values corresponding to acid deficiencies in the range 0.5 to $1.0\underline{N}^b$ at 24°C were determined for 2.2M aluminum nitrate solutions.

Acid-deficient 2.2M aluminum nitrate solutions were prepared by adding the appropriate amount of concentrated ammonium hydroxide to a given volume of 2.3M aluminum nitrate solution and then shaking the resulting slurry until all solids dissolved. The solids dissolved readily.

Figure 2 shows the pH values corresponding to acid deficiences from 0 to $1.0\underline{N}^b$ for 2.2M aluminum nitrate solutions. The portion of the curve below $0.2\underline{N}^b$ was reproduced from the Redox Technical Manual [7]; the portion of the curve in the acid deficiency range 0.54 to $1.0\underline{N}^b$ shows experimental values obtained from this investigation.

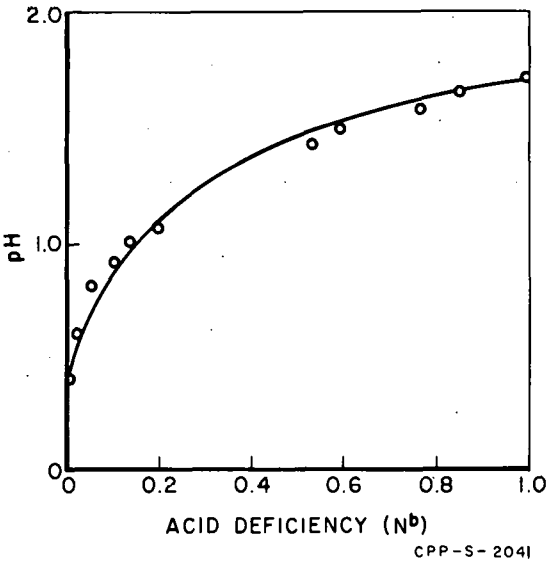

Fig. 2 Acid deficiency vs pH for 2.2M aluminum nitrate solution at 24°C.

Acid deficiencies corresponding to pH values of aluminum nitrate solutions of concentrations different than 2.2M can be predicted by the use of the 2.2M curve in conjunction with curves found in the Redox Technical Manual. As aluminum nitrate solutions become less concentrated in aluminum, the pH value for a given acid deficiency becomes greater. Thus, although uranium would not precipitate from a 2.2M aluminum nitrate solution with an acid deficiency of $1.0\underline{N}^b$, a 1.2M aluminum nitrate solution having an acid deficiency of $1.0\underline{N}^b$ would have a pH of about 2.9 and uranium could precipitate from such a solution. When used scrub solutions are recycled back to the extraction column and combined with the extraction column feed, the aluminum nitrate of the scrub solution is diluted and usually

becomes less acid deficient. However, if conditions were such that the scrub was diluted without sufficient decrease in acid deficiency (when combined with the extraction column feed), the precipitation of ammonium diuranate is quite possible.

2.2 Density of Basic Aluminum Nitrate Solutions (J. W. Codding)

During a study of the dibasic aluminum nitrate (Diban) process for U-Al alloy fuels, the densities of various basic aluminum nitrate solutions were measured as a function of solute concentration and degree of aluminum hydrolysis. Solutions were prepared ranging from 1.27M to 4.25M in aluminum concentration and from 0.45 to 2.08 for the $OH/_{Al}$ ratio.

A density equation of the form

$$D_{25} = \rho_{25} + K_{25} C_{Al}$$

was applied to these data. In this formula, D_{25} = solution density at 25°C, ρ_{25} = water density at 25°C, C_{Al} = molar concentration of total aluminum, regardless of its hydrolysis, and K_{25} is the density factor. The effect of aluminum hydrolysis on the density factor can be obtained by plotting K_{25} vs $OH/_{Al}$. This effect is essentially a linear one, with

$$K_{25} = K_{25}^{o} + S\left(\frac{OH}{Al}\right)$$

where $K_{25}^{o} = 0.160$ and the slope $S = -0.0415$. The density correlation then is of the form

$$D_{25} = \rho_{25} + \left[K_{25}^{o} + S\left(\frac{OH}{Al}\right)\right] C_{Al} \qquad (1)$$

where $\rho_{25} = 0.9971$, $K_{25}^{o} = 0.160$, $S = -0.0415$.

This equation, at zero hydrolysis $\left(\frac{OH}{Al} = 0\right)$, reduces to

$$D_{25} = 0.9971 + 0.160\ C_{Al}$$

which does not quite match the familiar equation for aluminum nitrate solutions

$$D = 1.000 + 0.155\ C_{Al}$$

Consequently, the data were examined using a value of 1.000 for ρ (water density at 4°C). This treatment yields a K_4^{o} value of 0.1575. Though this is still somewhat above the generally accepted value, the resulting equation

$$D_{25} = 1.000 + \left[0.1575 - 0.0408\left(\frac{OH}{Al}\right)\right] C_{Al} \qquad (2)$$

represents the system as well as Equation (1).

Since the relationship between density factor (K) and degree of hydrolysis $(\frac{OH}{Al})$ is a linear one, any solution of basic aluminum nitrate can be thought of as a two-solute system, ie, a mixture of $Al(OH_3)_3$ and $Al(OH)_2NO_3$. For such a case, the density equation is of the form

$$D = \rho + K_2 C_{Al(OH)_2NO_3} + K_1 C_{Al(NO_3)_3} \qquad (3)$$

where $C_{Al(NO_3)_3} + C_{Al(OH)_2NO_3}$ = total aluminum concentration,

and where the values of K_1 and K_2 depend on whether ρ is chosen as 0.9971 or 1.000. Appropriate values of K_1 and K_2 for Equation (3) are listed in Table VII.

TABLE VII

DENSITY FACTOR VALUES FOR VARIOUS WATER DENSITIES

ρ	K_1	K_2
0.9971	0.160	0.077
1.000	0.1575	0.076

Measurement of aluminum concentration and solution density, or of acid deficiency and solution density, is sufficient to define the system using any of the three density equations presented above.

3. GENERAL AQUEOUS STUDIES

3.1 OMRE Fuel Cleaning and Dissolution (R. D. Fletcher, Problem Leader; M. E. Jacobson, L. A. Decker)

3.11 Coating Removal. Fuel elements removed from the OMRE reactor for reprocessing are coated with a carbonaceous degradation product of the terphenyl moderator-coolant used in the reactor. It has been postulated that this interfering layer must be removed prior to processing if the dissolution is to proceed at a satisfactory rate and if solids are to be kept from subsequent process steps.

Studies of coating removal by treatment with Turco 4502 were made on samples cut from fuel element plates from Core 2 discharged from the OMRE reactor. One lightly-coated, one medium-coated, and one heavily-coated sample were heated at 180°F for two hr in Turco 4502 solution. Coating removal appeared complete on the lightly coated sample but not complete on the medium

or heavy ones. A medium-coated sample treated in a like manner in Turco Smut-Go 2 showed no apparent change in the coating.

The three Turco 4502 solutions were filtered and the residues analyzed for iron and manganese. Iron content of the solids ranged between 3.6 and 5.2 percent. Manganese varied between 11 and 25 percent. No iron was detected in the three filtrates. The iron in the coating was identified by X-ray diffraction as iron-carbide, $Fe_{20}C_9$.

Studies were conducted on coating removal from pyrolytically prepared heat exchanger tubes and wires. The samples were treated initially by boiling in Turco 4502. If coating removal was not satisfactory, the samples were heated to 500°C. The samples are described and cleaning results are summarized in Table VIII.

TABLE VIII

DESCRIPTION AND CLEANING OF
PYROLYTICALLY FOULED HEAT EXCHANGER SURFACES

Sample Description			Fouling Conditions			Cleaning Results	
Type	(a) No. of Specimens	Description	Surface Temperature °F	Time of Exposure Hr	Fouling Coat	Turco 4502	500°C in Air
1	11	Split Tubes 1/2-in. diam x 8 in.	900-1050	6-8	light	ok in 2-3 hr	—
2	5	Wires 0.1-in. diam x 1 in.	1050	10-67	heavy	not in 6 hr	ok in 2 hr
3	15	Split Tubes 1/2-in. diam x 1 in.	825-1011	173-3760	heavy	not in 6 hr	ok in 2 hr

(a) Type 1 samples from Phillips Petroleum Company
Type 2 samples from California Research Corporation
Type 3 samples from Atomics International

It has been concluded that the Turco 4502 treatment is only partially effective in removing or reducing the thickness of the hard scale on the fuel. It may be entirely adequate for lightly fouled surfaces. Heating at 500°C in air is essentially completely effective in removing the films.

For process application each method for film removal has disadvantages. The aqueous Turco 4502 treatment produces both a liquid waste and a solid or a thin slurry. The solid will scavenge the radiocolloids, which are present as activation products or fission products from cladding failures. If the precipitate is separated from the solution in the cleaning loop it will decontaminate the cleaning solution. In the process where the film is oxidized in air there will be a problem of contaminated off-gas disposal.

The completed experimental results for this program are being published in a topical report.

3.12 Dissolution of Fouled OMRE Plates. Although removal of the degraded terphenyl coating from irradiated organic-cooled reactor fuel elements prior to dissolution may be the preferred approach at this time, it appeared that certain dissolution systems might adequately penetrate the coating to secure dissolution of the fuel, and the resultant solids might be tolerated in the solvent extraction system. Therefore, a few preliminary experiments were performed on OMRE plate coupons to explore this possibility.

Electrolytic Dissolution. A heavily-fouled OMRE Core 2 plate was dissolved electrolytically in 8M nitric acid at four volts direct current and a current density of 1 amp/cm^2. The product solution, which was 6.3N acid, was contacted with 10 percent TBP extractant in the emulsion tester [8]. Finely-divided residue from the coating was present in the system. The coalescence time was about 40 sec which indicated that excessive emulsification would not occur during column operation; 300 sec is considered [8] to be the break point for acceptable coalescence performance.

Sulfuric Acid Dissolution. A medium-fouled OMRE Core 2 samples plate was dissolved in boiling 6.5M sulfuric acid. This was followed by dissolution of the uranium dioxide in nitric acid added to the sulfate solution. This dissolver product was adjusted for solvent extraction and the coalescence time determined. A value of 65 sec was obtained which suggested that no emulsion problem would be created due to the solids.

In both cases the dissolution reagent was observed to penetrate the carbonaceous coating and not just react at the cut edges. The results of these preliminary tests indicated that at least one type of organic fouling was readily penetrated by the regular dissolution reagents and that the resultant dissolver product gave column feeds which did not form stable emulsions even though solids from the coating were present. The solids content of these solutions was much less than that of the U-Al fuel which contained four percent silicon and which was satisfactorily processed in the ICPP. Further laboratory development, and eventually plant tests, would be required to demonstrate that cleaning of the fuel prior to dissolution is not needed to avoid serious plant problems.

3.2 Dissolution of Irradiated Thorium by the Thorex Process (R. D. Fletcher, Problem Leader; M. E. Jacobson)

A series of batch dissolutions of irradiated thorium slugs has been completed in the CPP Multicurie Cell [9]. These dissolutions were performed to secure analytical samples from irradiated specimens as a part of the MTR Technical program in fuel element development. Three dissolutions of two slugs each were made. The aluminum-clad slugs, 1-1/2 in. in diameter and 6-1/2-in. long, irradiated up to 3.2 mg of uranium-233/g of thorium, were declad in 6M nitric acid-0.005M mercuric nitrate. The thorium was dissolved in 15M nitric acid-0.04M hydrofluoric acid. Although acid addition and heating proceeded at the maximum safe rate, dissolution to approximately 280 g/l thorium took 26 to 30 hr. A small amount of solids appeared in the dissolver product solution but this essentially all dissolved when the solution was diluted to 140 g/l.

III. ELECTROLYTIC DISSOLUTION SYSTEMS

(Section Chief: K. L. Rohde, Chemistry;
Group Leaders: H. T. Hahn, D. W. Rhodes, R. D. Fletcher)

The dissolution of stainless-steel-uranium metallic fuels by electrolytic means is under investigation at the ICPP. Current work on this project includes development of chemical flowsheets for Nichrome-containing fuel, such as the HTRE fuel, and evaluation of possible electrical insulating materials for use in a pilot-plant electrolytic dissolver.

Extensive work has been reported in previous quarterly progress reports on the electrochemistry of type 304 stainless steel in nitric acid. A brief study is reported on the anodic overvoltages for the electrolytic dissolution of Nichrome in nitrate solutions. Secondary passivation was not observed in nichrome dissolution, as contrasted with type 304 stainless-steel dissolution. Concentration polarization is present under some conditions for current densities above 1 amp/cm^2 but can be eliminated in all practical dissolver systems by operating at 70°C.

In studies on the electrolytic dissolution of alloys of iron, nickel and chromium (APPR fuel), physical properties including density, stability to precipitation, and viscosity of the solutions are reported.

Investigation of materials suitable for electrical insulation in an electrolytic dissolver, and resistant to chemical attack and radiation damage, indicates that polyethylene is superior to other materials tested to date. Additional materials are being evaluated.

1. ELECTROLYTIC DISSOLUTION OF NICHROME AND STAINLESS STEEL

1.1 The Electrochemistry of Nichrome (J. R. Aylward, Problem Leader; E. M. Whitener)

Electrolytic dissolution in nitric acid shows promise as a head end treatment for reprocessing HTRE fuel element materials containing Nichrome. From previous work on the electrolytic dissolution of iron, nickel and chromium alloys, the general behavior of Nichrome dissolution could be predicted. For this reason, only a limited number of experiments were required to confirm the prediction and to establish optimum operating conditions for Nichrome dissolution.

The potential-current density curves follow the Tafel equation ($\eta = a + b \log I$) where the slope(b) is equal to 0.038 volts for all the solutions and temperatures studied. Hence, it may be assumed that the dissolution mechanism is invariant in the Tafel region under these conditions. In some cases a limiting current density due to a product concentration polarization is reached at high current densities, but in all cases the Tafel equation is obeyed up to currents of 10^{-1} amp/cm^2. The prediction that secondary passivation (as observed in stainless-steel dissolution) would be absent was verified. This prediction was based on the relatively high chromium content of Nichrome.

The effect of solution composition on the dissolution rate (current density) at constant temperature is shown in Figures 3 and 4. Hydrogen ion was found to have no effect in the Tafel region (Figure 3). Isolation of its effect on the limiting current density was difficult since it is experimentally impossible to change either the hydrogen or Nichrome cation concentration singly without changing the nitrate concentration. In this work it was desired to maintain the nitrate concentration constant in all experiments. Therefore, any influence of either hydrogen or Nichrome cations could not be determined independently without introducing another anion whose influence on the polarization curves also would be unknown. The effect of hydrogen ion may be inferred from the fact that the reaction rate in the Tafel region is independent of hydrogen ion concentration. It is logical to assume that the over-all reaction remains the same (with the rate independent of H^+ concentration) in the limiting current density region. The only difference is that the rate-determining step changes from activation controlled (Tafel region) to the transport of reaction products away from the metal-solution interface (limiting current density region). Also, since the rate of mass transport of product from the anode would be a direct function of the product concentration gradient, the influence of hydrogen ion would be at most a second order effect. It is therefore concluded that the difference in the values of the limiting current density observed in Figure 3 is due to the Nichrome cations.

Figure 4 shows that at constant potential the current density increases with decreasing nitrate ion concentration in both the Tafel and limiting current density regions. The behavior of the limiting current density with solution compositions shown in Figures 3 and 4 is typical of anodic concentration polarization. The substitution of Cr^{+6} for Cr^{+3} had no effect on the polarization curves.

The effect of temperature on the dissolution rate at constant solution composition is shown in Figures 5 and 6. From these data the heat of activation $\Delta H^{\ddagger}$ in the Tafel region (at 1.1 volts) was calculated to be 13.2 kcal/mole. The value of the limiting current density is increased with increasing temperature and, in a typical dissolver solution (containing 116 g/l of Nichrome) at 70°C, concentration polarization is absent at current densities up to 4 amp /cm^2 (Figure 6). However, in 10M nitric acid at 70°C concentration polarization

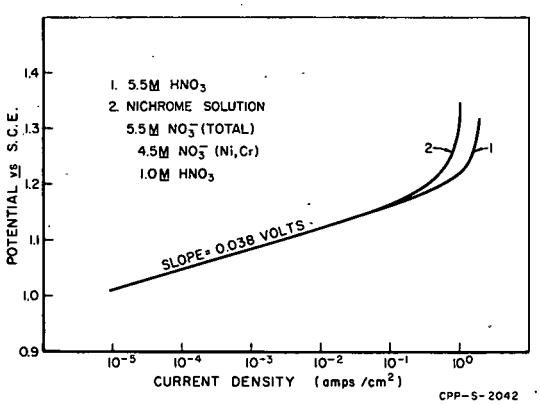

Fig. 3 Effect of hydrogen ion on the anodic dissolution of Nichrome in the transpassive region at 25°C.

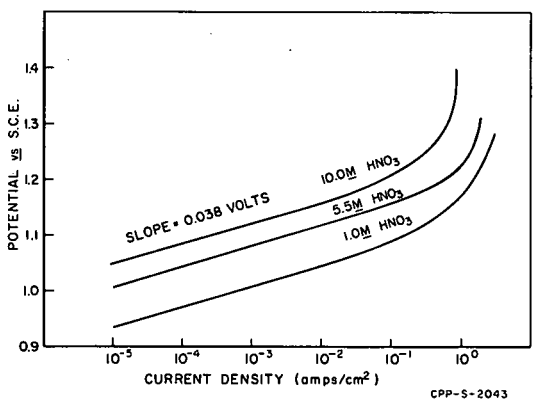

Fig. 4 Effect of nitric acid concentration on the anodic dissolution of Nichrome in the transpassive region at 25°C.

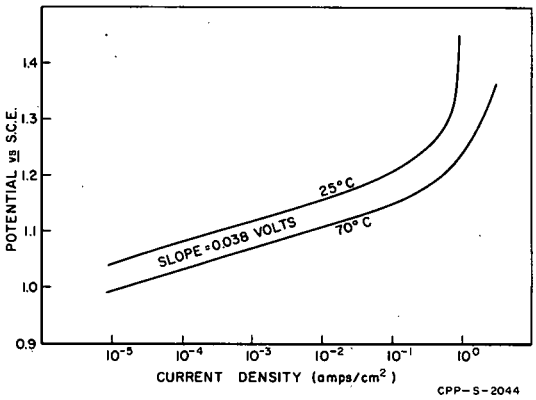

Fig. 5 Effect of temperature on the anodic dissolution of Nichrome in the transpassive region in 10M HNO_3.

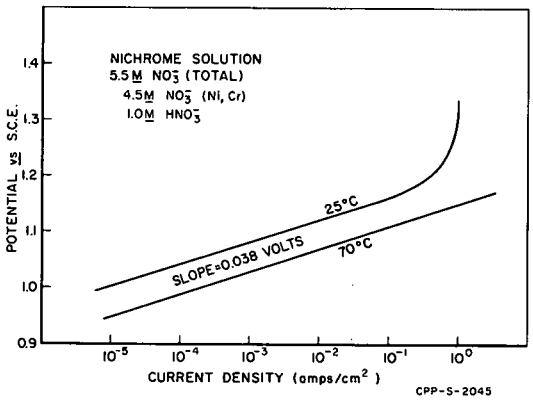

Fig. 6 Effect of temperature on the anodic dissolution of Nichrome in a typical electrolytic dissolver solution.

still is present to some degree at the currents of operating interest. This is due to the higher nitrate ion concentration.

In the limiting current density region the reaction rate is controlled by the mass transport of reaction products away from the metal-solution interface. Therefore, the dissolution rate can be increased by agitation, higher temperature, and the use of solutions in which nickel and chromium nitrates have a higher solubility. It is concluded that an operating temperature of 70°C is sufficient to eliminate concentration polarization, provided the nitric acid concentration is less than 10M.

1.2 Physical Properties of Iron, Chromium and Nickel Nitrate Solutions (J. W. Codding, Problem Leader; C. E. May)

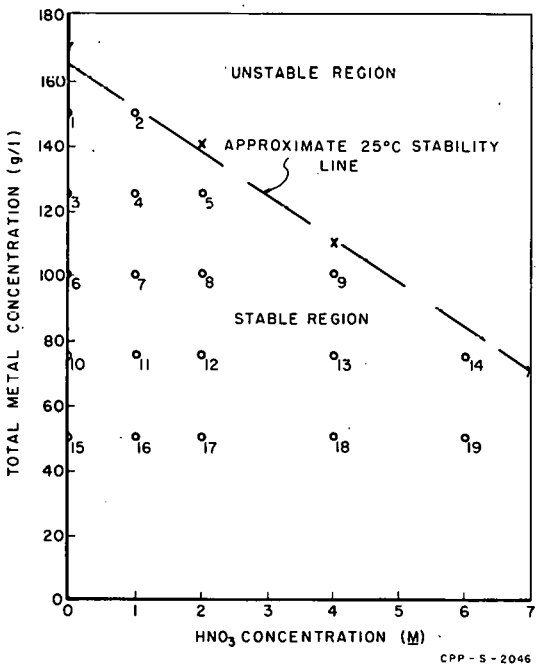

Fig. 7 Stability of APPR fuel dissolver solution.

The densities and viscosities of a series of stable solutions in the chemical system, ferric nitrate-chromium nitrate-nickel nitrate-nitric acid, were determined at 25°C. These data plus the solution stability data were used for the preparation of a chemical flowsheet for APPR stainless-steel fuel.

1.21 Solution Compositions. A matrix of solutions of iron, chromium and nickel nitrates and nitric acid was set up as shown in Figure 7. Specific compositions are indicated by the numbered open circles. The metal ions were present in fixed proportions approximating those of an APPR fuel dissolver product solution. For example, the 100 g/l solution contained 65 g/l iron, 18 g/l chromium, 9 g/l nickel, and 8 g/l uranium.

1.22 Solution Stability. Exploratory experiments on solution stability had indicated that solutions of compositions

indicated by the crosses on Figure 7 were unstable or metastable (they crystallized immediately upon seeding). Solutions of compositions indicated by the open circles were observed and found to be stable for longer than two months at 25°C. The high solubilities, especially at the lower acid concentrations, offer opportunity for the use of very concentrated flowsheet solutions.

1.23 Density. An attempt to obtain a correlation of the density and composition in a simplified form involving constant coefficients yielded very poor agreement between calculated and experimental densities. Accordingly a model of the form

$$D_{25} = 0.997 + (K_1 - S_1 C_{NO_3}) C_M + (K_2 - S_2 C_{NO_3}) C_H \quad (1)$$

was applied to the data. In Equation (1) K_1 and K_2 are infinite dilution density factors for the metals and nitric acid, respectively, and S_1 and S_2 are the slopes of K vs C_{NO_3} for each constituent. C_{NO_3} is the molar concentration of total nitrate and C_M and C_H are the molar concentrations of metals and acid, respectively. The values for the constants for this particular system were $K_1 = 0.00316$, $K_2 = 0.0345$, $S_1 = 0.000030$ and $S_2 = 0.000040$, applied to metal. This correlation gave agreement between calculated and experimental values of $\pm$ 0.003 g/cc or less.

1.24 Viscosity. The viscosities (25°C) of the solutions shown in Figure 7 varied from 1.5577 centipoises at zero acid and 50 g/l stainless steel to 7.4115 at 1M acid and 150 g/l stainless steel. These viscosities are not excessively high for column operation since 1.5M aluminum nitrate (about 3.3 centipoises) is used as aqueous feed for solvent extraction in pulsed columns, and 2M aluminum nitrate (6.2 centipoises) is used as scrub in packed columns at ICPP.

1.25 Further Data. Additional stability, electrical conductivity, density, and viscosity data have been obtained for the more general system in which the concentration of the different metal ions was varied independently. These data and the details of the system as discussed above are being presented in a topical report.

2. MATERIALS OF CONSTRUCTION IN ELECTROLYTIC SYSTEMS

(R. D. Fletcher, Problem Leader; L. A. Decker)

2.1 Preliminary Chemical Tests

Styron 475-6034, a polystyrene sample furnished by Auburn Plastics, was tested in electrolytic dissolver product, 1M HNO_3-75 g/l stainless-steel components, at the boiling point for 72 hr. A slight warping occurred upon heating, probably as a result of molded-in stress. Weight gain was about 0.5 percent; no swelling or disintegration occurred. Sample became stiffer but apparently no more brittle.

Stycast 2741, supplied by Emerson and Cuming, Inc., also was tested in the dissolver product solution at the boiling point for 72 hr. The samples were completely disintegrated at the end of the test.

Nucerite-coated stainless steel, a ceramic coating supplied by Pfaudler Co., also was tested as above. No change was observed at the end of the test.

2.2 Irradiation Tests

In the previous quarterly progress report [10], the irradiation of four chemically-resistant plastics to 10^9 r total dose was reported. Of these only the Marlex* polyethylene did not suffer excessive cracking, spalling, or disintegration. Impact and compressive yield strength measurements made on the Marlex are shown in Table IX.

The compressive yield strength was apparently unaffected by the irradiation but the impact strength decreased to only 15 percent of the original after a total irradiation dose of 10^9 r gamma. While these values of impact strength can be used only for comparison and are not suitable for design purposes, it is interesting to note that the impact strength for Marlex is as good after a total dose of 10^9 r as for many other plastics which have not been exposed to radiation.

TABLE IX

EFFECT OF IRRADIATION ON THE PHYSICAL PROPERTIES OF MARLEX POLYETHYLENE

(Irradiated in 1M HNO_3 - 75 g/l Stainless-Steel Solution at 101°C).

Specimen	Unirradiated	10^8 r Total Dose	10^9 r Total Dose
	Izod Impact Strength, ft-lb /in. of notch		
1	3.79	3.73	0.56
2	3.23	3.50	0.55
3	4.00	3.31	0.50
Average	3.67	3.51	0.54
	Compressive Yield Strength, psi		
1	2910	2950	2820
2	2960	2770	2940
3	2790	2890	2910
Average	2890	2870	2890

* Trademark of Phillips Petroleum Co.

IV. NEW WASTE TREATMENT METHODS

(Section Chief: K. L. Rohde, Chemistry; Group Leader: D. W. Rhodes)

1. DISPOSAL OF LOW-LEVEL RADIOACTIVE WASTES

(M. W. Wilding)

Laboratory work was initiated under a special arrangement with IDO-AEC to investigate the possibility of using locally-available natural earth materials as ion exchangers for the removal of radioisotopes from low-level radioactive wastes at the National Reactor Testing Station. The initial phase of this investigation consisted of measuring important chemical and physical characteristics of several natural earth materials.

The materials used in this investigation included four different lignitic samples and three clay-like materials obtained from Eastern Idaho deposits. The clay-like materials were either distributed in small amounts throughout one of the lignitic materials or occurred in a deposit overlying this material. The cation exchange capacity of these materials, determined by a standard procedure [11], varied from about 0.1 to 1.0 milliequivalents/g of solid. The highest exchange capacity was obtained for a lignitic material, and this value was about twice that of the next best material, also a lignite. Consequently, subsequent tests were confined to the high exchange capacity lignite. Additional tests showed that the exchange capacity is independent of particle diameter over the range 0.05 to 1.0 mm, suggesting that the chemical and structural composition of the material is uniform.

The removal of cesium and strontium from solution by adsorption on the lignitic material was determined as a function of time and pH. A batch equilibrium technique was used in which the solid and liquid containing one mg/l of cesium or strontium traced with cesium-137 or strontium-85 were equilibrated by shaking on a mechanical shaker; sodium hydroxide or nitric acid was used to adjust the pH. The distribution of the cesium or strontium between the solid and the liquid was then determined by measuring the concentration of radioisotopes in a well-type scintillation counter.

The results of the rate experiment, shown in Figure 8, show that the exchange reaction is very fast for both cesium and strontium.

The influence of pH is shown in Figures 9 and 10. Maximum adsorption for both cesium and strontium occurs at a pH between 6 and 8. This pH range is readily achievable in low-level wastes, and the distribution coefficients are sufficiently high to suggest that this material is a good potential candidate for the removal of radioisotopes from low-level radioactive wastes.

Additional locally-available materials will be studied and the materials exhibiting the highest potential for removing fission products from solution will be studied in detail.

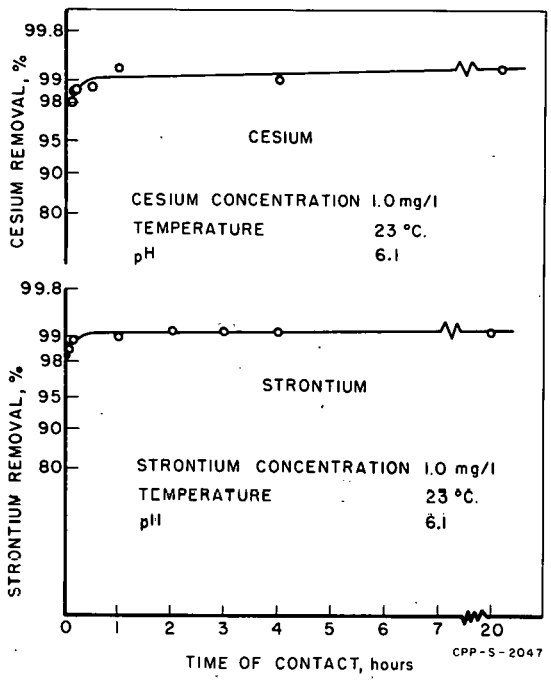

Fig. 8 Removal of cesium and strontium from solution as a function of time.

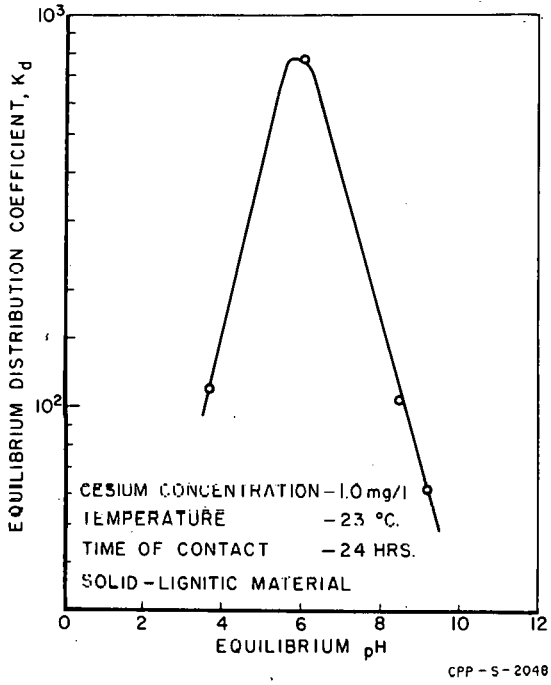

Fig. 9 Equilibrium distribution of cesium as a function of pH.

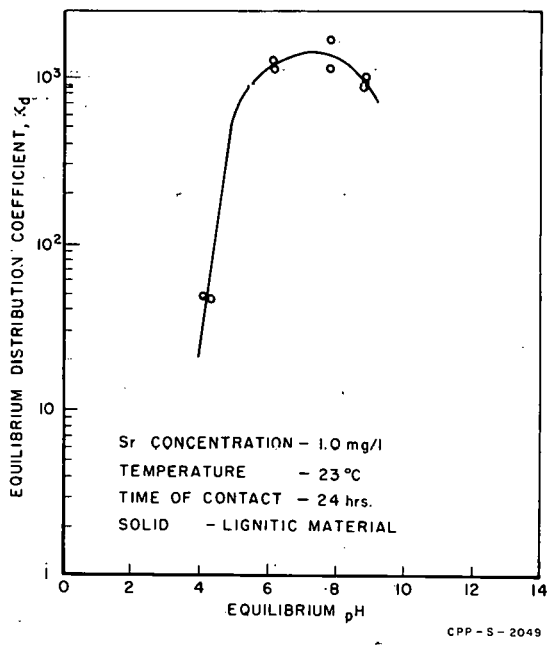

Fig. 10 Equilibrium distribution of strontium as a function of pH.

V. WASTE CALCINATION DEVELOPMENT AND DEMONSTRATION

(Section Chiefs: R. A. McGuire, Development Operations; K. L. Rohde, Chemistry; J. I. Stevens, Development Engineering)

Laboratory and pilot plant studies of the fluidized bed calcination process for reduction of high-level wastes to a granular, free-flowing solid have been underway since 1955 at the ICPP. Early studies were conducted in 3-in. and 6-in.-diam units; currently, a 12-in.-diam, electrically-heated unit and a 24-in.-square, NaK-heated unit are used for pilot plant studies with non-radioactive material. A 48-in.-diam Demonstrational Waste Calcining Facility (DWCF) has been built for demonstration of this process with full-level wastes; the first phase of cold-startup testing of the DWCF is underway.

Although exploratory studies have been made to demonstrate the feasibility of the fluidized bed calcination process for stainless-steel and zirconium fuel wastes, the overwhelming majority of the work to date has been concerned with wastes from the processing of uranium-aluminum alloy fuels. A typical waste of this type contains 1.74M aluminum nitrate, 0.6M nitric acid, 0.01M mercuric nitrate, 0.04M sodium nitrate, fission products, and other minor components. Studies to date have shown that calcination between 350 and 550°C, with a superficial fluidizing gas velocity of about 1 ft/sec can lead to a suitable product at reasonably high capacity.

Feed rates up to 120 l/hr have been achieved in the 24-in.-square pilot plant calciner, the capacity apparently being limited by the heat transfer area provided. Volume reduction factors from aqueous waste to bulk-stored solids of from 8 to 24 have been demonstrated. A desirable product has been defined as one having a mass median diameter between 0.3 and 0.6 mm, a low intra-particle porosity, and a low attrition rate. Particle size has been found to be controllable by variation in the nozzle air-to-liquid ratio, and particle porosity has been found to vary directly with calcination temperature and feed aluminum concentration.

The principal remaining problem is determination of the factors affecting the rate of conversion of the originally-formed, attrition-resistant amorphous form of alumina to the easily-attrited alpha form. Four variables were found to be of prime importance in this regard: temperature, composition of the gaseous environment, method of alumina formation, and sodium content of the feed solution. Basic aluminum nitrates were studied as possible calcination intermediates. The structure of the amorphous material was studied by examining radial distribution data from X-ray diffraction. The possible effect of additives has been considered, and the distribution of crystalline material in individual particles of calcine is being determined.

Studies were continued in the 12-in. and 24-in. pilot plant calciners and in the 48-in. Demonstrational Waste Calcining Facility (DWCF). Pilot plant studies indicated no significant effect of mercury in the feed and showed a direct relationship between feed sodium content and alpha alumina formation rate.

Process flowsheet preparation and preliminary equipment design were started for a hot pilot plant installation to study the pot calcination process.

1. LABORATORY INVESTIGATIONS

1.1 Laboratory Studies of Alumina Phase Transformation at the ICPP (D. W. Rhodes, Problem Leader; R. F. Murray)

The formation of alpha phase alumina from the amorphous phase during calcination of aluminum nitrate-nitric acid wastes in a fluidized bed calciner is being investigated on a laboratory scale. Methods for preventing the growth of alpha alumina and encouraging the formation of amorphous alumina in the fluid bed are needed because the alpha form undergoes severe attrition in the calciner, resulting in excessive solids loading of the off-gas cleaning equipment.

1.11 Experimental Methods and Equipment. The laboratory experiments were performed either in a static test unit or in a small fluidized bed unit. In the static test unit [12], heated nitric acid and water vapors were mixed with heated air to simulate the fluidized bed calciner atmosphere, and the mixture was passed through alumina samples. The fluidized bed unit was constructed of Vycor glass and permitted preparation of calcined alumina under a wide variety of conditions for further testing in the static test unit.

The crystal composition of the alumina, after treatment in either type of equipment, was determined by X-ray diffraction. This technique is adequate to detect alpha alumina in quantities greater than five weight percent.

1.12 Discussion. The results of several different experiments in the static test unit are reported herein. A sample of material IV-A [1], a calcined material from an earlier pilot plant run containing less than five percent alpha alumina, was used as a control in each experiment. This material is known to convert to about 60 to 70 percent alpha alumina during heating in the static test unit in an air-water-nitric acid atmosphere for three days [1].

On heating material from 24-in. pilot plant calciner Run 20 (a very low sodium material) for three days at 500°C in an atmosphere of air and water vapor, no alpha or gamma alumina was formed; control material IV-A contained 13 percent alpha and a trace of gamma alumina at the termination of the experiment. These results indicate that the method of preparation of the starting material is important for the conversion to gamma as well as alpha alumina, particularly since an earlier experiment with a different starting material (<0.2 percent Na, <5.0 percent alpha, produced in the pilot plant at 500°C) produced large quantities of gamma alumina under similar conditions.

On a second test, using a water-air atmosphere with calcined alumina from various pilot plant runs as starting materials, alpha alumina formed in samples which had been shown previously to be alpha formers in a nitric acid atmosphere. However, the alpha alumina formed in the air-water vapor atmosphere was only one-third to one-half that formed previously in the air-water vapor-nitric acid vapor atmosphere. On a third test in which only air (no water or nitric acid vapors) was passed through the system, only sample IV-A showed any phase changes after three days of heating at 500°C, and this sample contained only five to nine percent alpha alumina.

These three experiments clearly demonstrate that very little alpha alumina is formed by heating amorphous pilot plant product in air but that moderate amounts of alpha can be formed from "sensitive" starting material in an

air-water vapor atmosphere. Earlier laboratory experiments demonstrated that large amounts of alpha alumina can be formed if nitric acid vapors are added to the air-water vapor mixture.

In a different series of experiments, calcined alumina prepared in the laboratory fluidized bed calciner was heated in the static test unit for three days at 500°C in an atmosphere of air-water vapor-nitric acid vapor. Under these conditions the control (IV-A) material gave 70 percent alpha alumina. A maximum of 19 percent of the amorphous alumina from the laboratory fluidized bed calciner was converted to alpha alumina in these tests. This, however, was the first time that alpha alumina had been obtained from amorphous alumina produced in the laboratory from a liquid feed at moderate temperatures. Previous attempts using "boil-down" techniques, as contrasted with the fluidized bed calcination, had produced amorphous alumina which would not convert to alpha alumina under these conditions. However, the fluffy, irregular-shaped product produced in the laboratory fluid bed calciner has not simulated adequately the conversion from amorphous to alpha alumina obtained from material produced in the larger pilot plant units.

Samples of alumina from Runs 21 and 22 in the 24-in. pilot plant calciner were heated in the static test unit for one week at either 400 or 500°C in an atmosphere of air-water vapor-nitric acid vapor. These materials contained less than five percent alpha alumina prior to treatment in the laboratory unit. The results are shown in Table X.

TABLE X

CONVERSION OF AMORPHOUS ALUMINA TO ALPHA ALUMINA

(Heated in Air-Water-Nitric Acid Vapor for One Week)

Amorphous Alumina Source		Percent Alpha Alumina after heating	
(Pilot Plant Run No.)	(Hours after PP Run Initiation	(500°C)	(400°C)
21	116	20	67
21	138	28	73
21	226	32	81
21	358	63	83
IV A (control)	—	68	67
22	10	79	—
22	18	76	—
22	30	77	—
IV A (control)	—	66	—

The results in Table X clearly point out that the material produced during Runs 21 and 22 in the pilot plant calciner was capable of converting in large measure to alpha alumina under conditions slightly more favorable for alpha formation than apparently existed in the fluidized bed calciner. Furthermore, the potential of the material to convert to alpha alumina increased as the pilot plant run progressed. Although 400°C appeared to be a more favorable temperature for the conversion than did 500°C, the fact that the control (IV-A) experienced about the same conversion to alpha alumina at both 400 and 500°C suggests that this temperature dependency may have been peculiar to the alumina produced under the specific conditions prevailing for Run 21.

The rate of conversion of amorphous alumina to alpha alumina was studied during the test on material from Run 22. Samples from Run 22 contained 60 to 80 percent alpha alumina after only 18 hr heating in the static test unit in a simulated calciner atmosphere. After a total of 44 hr heating, very little, if any, increase in the amount of alpha alumina was observed. Apparently, the rate of conversion is very rapid, suggesting that factors other than residence time are very important in converting this particular material to alpha alumina.

The content of gamma alumina formed by heating Run 21 product was about four times as high in the samples containing 32 percent or less alpha alumina as in the samples containing 60 percent or more alpha. Conversely, the crystalline sodium nitrate content was three to four times as high in the high alpha alumina samples as in the samples low in alpha.

Samples of the overhead fines from the laboratory fluidized bed calciner were of particular interest. Overhead fines collected when the calcination conditions approached spray drying (very low fluidized bed level) produced an X-ray diffraction pattern the same as a pattern previously obtained from a solid material that had been dried from a solution of 8M dibasic aluminum nitrate. These results suggest that the dibasic aluminum nitrate compound may be an intermediate form produced during the calcination process.

1.2 Studies at Stanford Research Institute (C. M. Slansky, Project Liaison)

Under subcontract, the Stanford Research Institute currently is extending these laboratory studies along four lines of endeavor: First, a search is being made for intermediates present during calcination which would give an indication of the subsequent crystalline phases; second, the "structure" of amorphous alumina is being studied by examination of radial distribution data from X-ray diffraction measurements; third, the effect of various additives upon the crystallinity of the calcine is being studied; fourth, the distribution of crystalline material in individual calcined particles is being determined.

1.21 Transformation Studies. Aqueous solutions 1.6 to 1.7M in aluminum nitrate and with varying concentrations of HNO_3, $Al(OH)_3$, $NaNO_3$ and $Hg(NO_3)_2$ were evaporated to dryness and heated at 300°C for 8 to 16 hr in an open beaker. The dry alumina was amorphous to X-rays except for the samples containing $NaNO_3$ where crystalline $NaNO_3$ was observed. The water content was 0.7 ± 0.1 moles H_2O/mole Al_2O_3. Nitrate was approximately 0.3 ± 0.1 mole NO_3^-/mole Al_2O_3 and was independent of the presence or absence of 0.1M $NaNO_3$ in 1.7M $Al(NO_3)_3$. With 1.0M $NaNO_3$ in the acidic starting solution, the dry product gave a NO_3^-/Na_2O mole ratio of 2.24; with a basic aluminum nitrate and high concentrations of $NaNO_3$, the NO_3^-/Na_2O mole ratio in the dry alumina was 4.44, indicating a slow decomposition of basic aluminum

nitrate upon drying. The alumina produced at 300°C was then held at 400, 500 and 600°C in a furnace in a nitric acid-air atmosphere for 70 to 166 hr.

In no case was alpha alumina observed; small concentrations of gamma alumina were detected in most of the samples. Crystalline $NaNO_3$ was present in the high-Na samples and at 600°C was being converted to $NaAlO_2$. When NO_2 gas was added to the atmosphere in the furnace, the solid phases remained unchanged. The alumina showed a drop in water content at 600°C; 0.1 mole H_2O/mole Al_2O_3 was found in the absence or presence of one mole Na_2O/mole Al_2O_3. The mole ratio of nitrate to alumina was reduced to 0.001 at 600°C, showing conversion of $NaNO_3$ to $NaAlO_2$. At 400 to 500°C, the $H_2O/NO_3^-/Al_2O_3$ mole ratio was about $0.1/0.04 \pm 0.02/1$ in the absence of $NaNO_3$.

The 300°C dried solid was also heated at 400 to 500°C in a bomb under 150 psig pressure for 117 to 162 hrs. X-ray analysis showed the presence of a new anhydrous alumina with four lines whose d-values are 2.12, 1.40, 2.36, and 4.40. A small concentration of gamma alumina was noted, and the $NaNO_3$ pattern was intensified. The mole ratio of $H_2O/NO_3^-/Al_2O_3$ was approximately 0.4/0.1/1. A sample of amorphous alumina from the 24-in. pilot plant calciner formed major concentrations of alpha mono-hydrate (boehmite) at 400°C and with a mole ratio of 1.0/0.25/0.06/1 for $H_2O/NO_3^-/Na_2O/Al_2O_3$.

Differential thermal analyses have been found to be somewhat erratic between different samples of calcined alumina. In general, water is lost between 108 and 162°C, while the nitrate may be lost at the same or higher temperatures. The intensity of the peaks was very small for samples of amorphous or crystalline alumina from the 24-in. pilot plant calciner or the DWCF.

1.22 Radial Distribution Studies. Radial distribution data have been obtained on two amorphous pilot plant samples to determine whether the amorphous material is structurally related to alpha alumina. The first three interatomic distances in one sample were 1.9, 3.20, and 4.55 Å, and the corresponding distances in the other sample were 1.8, 3.15, and 4.50 Å. The 1.8 to 1.9 Å distance corresponds to the Al-O distances of 1.89 and 1.93 Å in alpha alumina. The O-O distance of 2.49Å and the Al-Al distances of 2.25 and 2.7 Å, which are in the alpha alumina structure, were not found; the 3.15 to 3.20 distance in the sample might be due to Al atoms surrounded by O atoms in a tetrahedral arrangement, while the 4.50 to 4.55 distance might be due to the packing of the tetrahedrons.

1.23 Effect of Additives. Additives to the aluminum nitrate waste solution prior to calcination might either stabilize the amorphous form or make it possible to control the kind and rate of crystal nucleation. For instance, boric acid might tend to flux the alumina and hold it in the amorphous state for a long time. Sodium is known to favor the formation of alpha alumina, possibly because beta alumina ($Na_2O \cdot 11Al_2O_3$) has a structure related to that of alpha alumina and might form a solid solution with alpha alumina. Similarly, potassium, rubidium, calcium, strontium, barium, and lead also probably would favor alpha alumina formation.

Another approach to the control of crystallinity is by favoring a denitration route whereby an intermediate such as boehmite is formed which does not transform to alpha alumina until 1050°C. The amorphous form of alumina might be maintained by the formation of B_2O_3 glass during calcination. Silicates, phosphates and other addition agents also might favor amorphous alumina.

Preliminary studies of the effect of additives have been made, using such additives as lithium, magnesium, calcium, potassium, iron, zinc, sulfate, phosphate, borate, and silicate. Batch calcination of these modified feed solutions at 300 to 450°C resulted, as usual, in generally amorphous material. Nitrates of sodium, potassium, and lithium were detected in the product. Furnace heating of the materials produced by batch calcination produced aluminates of lithium and zinc. Alpha monohydrate (boehmite) was found in many of the heated samples as was the "new" anhydrous alumina referred to earlier.

1.24 Electron Diffraction Studies. Electron diffraction studies of pilot plant-produced alumina amorphous to X-rays showed that this material also was largely amorphous to electrons and therefore did not consist of 10 to 100 Å crystallites.

A technique was developed for examining a diametrical cross-section through individual calcined particles. An orange-slice-shaped section was examined along the thin edge with a 25- to 50-μ-diam electron diffraction beam. This technique should be of considerable value in examining individual calcine particles produced in the fluidized bed calciners. The mechanism of crystal tranformation may be elucidated by observing whether the crystalline phase starts from the outer shell (due to a gas atmosphere) or is nucleated from certain layers or crystal centers. A number of particles have been examined but the results are not yet sufficiently complete to pose a mechanism for alpha transformation. These studies will be continued.

1.3 Intermediates During the Calcination of Aluminum Nitrate (C. M. Slansky; R. F. Murray)

In support of the basic study of alumina phase transformations, the chemical path by which aluminum nitrate is calcined to Al_2O_3 is being studied; it may be important in determining the crystalline form that the alumina will take.

After solution is injected into the calciner, all evidence points to the early formation of an amorphous form of Al_2O_3 which contains relatively small concentrations of water, the minor component sodium nitrate, and an excess residue of nitrate ion. The rate of conversion of amorphous to alpha alumina is slow, usually taking of the order of days to convert to alpha in the presence of low concentrations of $NaNO_3$ at 400°C. The time factor is important since the residence time in the bed of the DWCF is also of the order of days, and there is little chance of reducing the residence time of a particle in the bed below a value of about 30 hr.

During the development of the Diban process for the recovery of uranium from U-Al alloy fuels, aluminum was dissolved in a deficiency of nitric acid to a solution composition of 8M $Al(OH)_2NO_3$. The 8M solution rapidly converted to a glassy solid while a 4M solution started precipitation after several months of standing at room temperature.

The solids from the Diban process studies were found to be crystalline basic aluminum nitrate hydrates and were investigated as possible intermediates in the calcination process.

1.31 Diban Dihydrate - $Al(OH)_2NO_3 \cdot 2H_2O$. The precipitate from the 4M solution of $Al(OH)_2NO_3$ was filtered, washed with water, and air-dried under

vacuum. The mole ratio of $Al/OH^-/NO_3^-/ H_2O$ was found to be 1/1.8/0.8/2.3. When dried at 100°C, the water content dropped to 2.07 moles/mole Al. Based on this and other analyses, the composition is considered to be $Al(OH)_2NO_3 \cdot 2H_2O$.

The X-ray pattern of $Al(OH)_2NO_3 \cdot 2H_2O$ is given in Table XI.* Broadening of the diffraction lines indicates small crystal size. The material is insoluble in water and in pH-5 oxalate media.

1.32 Anhydrous Diban - $Al(OH)_2NO_3$. Samples of $Al(OH)_2NO_3 \cdot 2H_2O$ were heated at 200 and 300°C for 16 and 23 hr, respectively. The material at 200°C gave an analysis corresponding closely to $AlO_{1.1}(NO_3)_{0.78} \cdot 1.1H_2O$. An X-ray pattern of this compound is given in Table XI under the heading of $Al(OH)_2NO_3$. The compound was found to be very hygroscopic, a pale yellow color, and to contain 0.42 percent NO_2^-. The nitrite content is a small fraction of the total nitrogen but may be the source of the yellow color. A hygroscopic solid has not been reported in the various calcination studies; the physical properties of this intermediate may be important in particle build-up in the calciner.

When heated for 23 hr at 300°C, Diban dihydrate loses 58.4 percent by weight and becomes amorphous to X-rays. The product analyzed 11.0 percent nitrogen as nitrate with only 0.036 percent nitrite. The material balance indicated the incomplete decomposition of $Al(OH)_2NO_3$ to Al_2O_3; ie, the 11 percent nitrate probably was from undecomposed $Al(OH)_2NO_3$. The weight loss and analysis could not be attributed to a simple dehydration to $AlONO_3$. More work is planned on this reaction.

1.33 Higher Basic Nitrates of Aluminum. In the evaporation of solutions of $Al(OH)_2NO_3$, there is some decomposition toward a composition of $Al(OH)_{2.5}(NO_3)_{0.5}$. The corresponding solution 8M in aluminum solidified at room temperature to a clear, glass-like solid amorphous to X-rays. A well-defined X-ray pattern of many lines was noted after the material had been stored in a closed container for months. The solid is being purified for further measurements of its composition. The crystalline solid is white and water insoluble; the X-ray pattern is given in Table XI. This solid is converted to an amorphous material upon further heating.

2. RESEARCH AND DEVELOPMENT IN THE PILOT PLANT
(B. M. Legler, Problem Leader)

Development studies continued in the 24-in.-square pilot plant calciner in an effort to determine the effects of mercury and sodium in the simulated waste feed solution on the formation of alpha alumina. In the first of two runs, Run 21, mercury was found to have no noticeable effect on alpha alumina formation or any other property; this run included periods of operation without mercury and others with 0.015M mercury in the feed. In Run 22, the concentration of sodium in the feed was shown to be an important factor in the formation of alpha alumina. During the approximately 360 hr of Run 21 and the first 64 hr of Run 22, no alpha alumina was formed with a feed containing 0.078M

* X-ray analyses were made by W. A. Ryder of the Spectrochemical Laboratory of the CPP Analytical Section.

TABLE XI

X-RAY POWDER DATA ON BASIC
ALUMINUM NITRATE CRYSTALLINE MATERIALS

$Al(OH)_2NO_3 \cdot 2H_2O$ [a]		$8_M\ Al(OH)_{2.5}(NO_3)_{0.5} \cdot XH_2O$ [a]		$Al(OH)_2NO_3$ [b]	
d-spacing (A°)	Relative Intensity [c] (I/I_1)	d-spacing (A°)	Relative Intensity [c] (I/I_1)	d-spacing (A°)	Intensity (I)
9.6	100 b	18.	34 b	11.	s
7.6	41 b	12.7	100	7.6	m
8.8	50 b	8.8	65	4.85	w
6.3	17 b	8.34	38	4.15	vw
5.90	58 b	7.78	38	1.98	m
4.00	66 b	6.55	15	1.74	w
3.67	17 b	6.32	34		
3.53	41 b	5.32	11		
3.13	25 b	5.00	27		
2.93	58 b	4.84	15		
		4.69	19		
		4.55	23		
		4.48	15		
		4.41	42		
		4.18	46		
		4.05	23		
		3.90	19		
		3.90	15		
		3.85	15		
		3.77	15		
		3.60	15		
		3.35	31		
		3.24	46		
		3.13	11		
		3.07	27		
		3.02	27		
		2.91	22		
		2.62	11		
		2.53	11		
		2.37	27		

(a) By Diffractometer

(b) By Debye-Sherrer Powder Pattern; s = strong; m= medium; w= weak; vw; very weak

(c) b denotes broad line

sodium. Twenty-four hr after the feed sodium concentration was raised from 0.078M to 0.25M, alpha alumina was detected in the product. During an additional 22 hr, the alpha alumina content increased to 17 percent. The feed sodium concentration was then reduced to 0.03M, and the alpha alumina decreased gradually to seven percent during the final 91 hr of operation. The alpha alumina content of fines collected by the primary cyclone was always close to that of the bed material.

Another objective of these runs was to test a boron carbide nozzle cap for erosion resistance. Details of this cap, which was used during Runs 21 and 22, are shown in Figure 11 along with those for a standard metal cap. No quantitative nozzle erosion data have been obtained, since, due to fragility of boron carbide, no attempt was made to remove the nozzle for measurement. Visual inspection, however, revealed only minor polishing. A nozzle air-to-liquid volume ratio of 600 was necessary for stable operation in both runs with this modified nozzle cap.

Construction of the 12-in.-diam calciner was completed during this period. Bench scale tests on fluidized bed distributor plates to determine the effect of air velocity on bed attrition indicated that plate hole velocities below 160 ft/sec do not cause excessive attrition of a high alpha alumina (55 percent) bed material. The results should be conservative for lower alpha alumina concentrations since attrition rate is directly related to alpha alumina content.

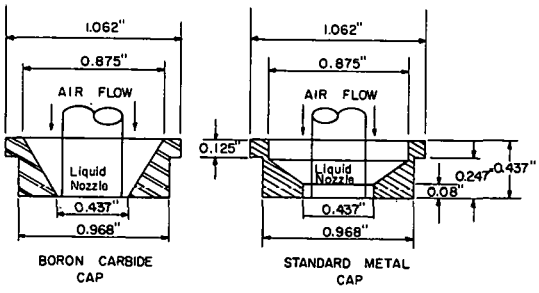

Fig. 11 Comparison of boron carbide and standard metal nozzle caps.

3. DEMONSTRATIONAL WASTE CALCINING FACILITY
(B. M. Legler, Problem Leader)

Operation of the Demonstrational Waste Calcining Facility (DWCF) was not possible during most of the quarter because of modifications being made by construction and maintenance forces. Among the modifications were changes in the calciner distributor plate, installation of a second NaK expansion tank, and installation of new pumps in the quench system.

The calciner distributor plate was modified by installation of bubble-cap inserts in the original fourteen 3/4-in.-diam air holes. These inserts reduced the air hole diam to 0.595 in. in order to provide a greater pressure drop across the distributor plate for more uniform fluidizing. Each insert was provided with a two-in.-diam impact plate located 3/8 in. above the air hole to distribute the fluidizing air more evenly and reduce bed attrition.

A temporary orifice meter, installed in one of the three feed nozzle lines, was calibrated with both water and aluminum nitrate solution. Observations of the feed nozzles in operation, from the temporarily-flanged manway at the top of the calciner, revealed unexplainable flow surges occurring in the feed system. The spray from the nozzles was erratic due to these feed fluctuations.

Occasionally a swirling during operation produced caking on the vessel wall concentric with the nozzle port; the presence of a fluidized bed probably would eliminate or at least greatly reduce this effect.

The objective of Run 4, which started late this period with sand as the initial bed material, was to determine the effects of equipment changes and of the starting bed on operability and on product properties. By the end of the period, the product contained about five percent alpha alumina and the percentage was increasing. The newly installed quench pumps (Lawrence) operated satisfactorily. Transport air blower service was marginal, however, due to the increased discharge pressure required by the more dense starting bed and by the increased pressure drop across the distributor plate.

4. POT CALCINATION

(B. R. Wheeler, Problem Leader)

Preparation of the process flowsheets and preliminary equipment design were started for a hot pilot plant installation to demonstrate the pot calcination process. This demonstration is being conducted in cooperation with the Chemical Technology Division of Oak Ridge National Laboratory. Probable location of the equipment is Cells 1 and 2 of the recently-completed Hot Pilot Plant. Space will be reserved for possible future coupling of a second type of calciner in the same installation.

VI. BASIC PROCESS STUDIES AND EQUIPMENT DEVELOPMENT

(Section Chiefs: K. L. Rohde, Chemistry;
(R. A. McGuire, Development Operations; J. I. Stevens, Development Engineering)

1. AIR PULSER OPERATING CHARACTERISTICS

(E. E. Erickson, Problem Leader; S. J. Horn)

Operating characteristics for the air-pulsers installed on the "B" and "C" columns of the ICPP continuous aluminum process have been predicted by analog simulation. The resulting curves, Figures 12 and 13, are for 30 percent organic-phase holdup. The predicted curves for the "A" column were presented previously [10]. The derivation of the equation, the methods of calculating coefficients, and the computer diagram have been described [13]. A simple square-wave driving function, previously shown to be an adequate representation of the pressure input in the "A" column simulation, was used for the "B" and "C" column calculations. A variable friction factor was used and it was assumed that a change in organic holdup from 30 percent to either 20 or 40 percent changed the pulse amplitude less than 10 percent as was the case for the "A" column.

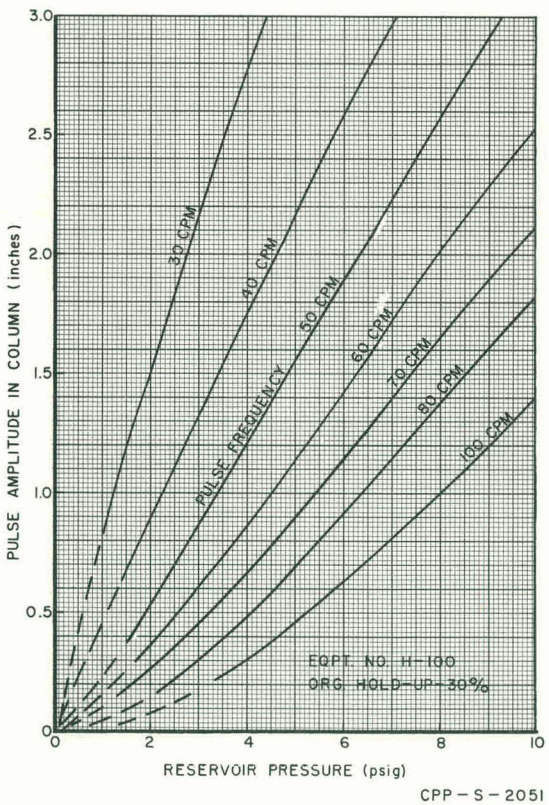

Fig. 12 Operating curves for 1-B column air pulser.

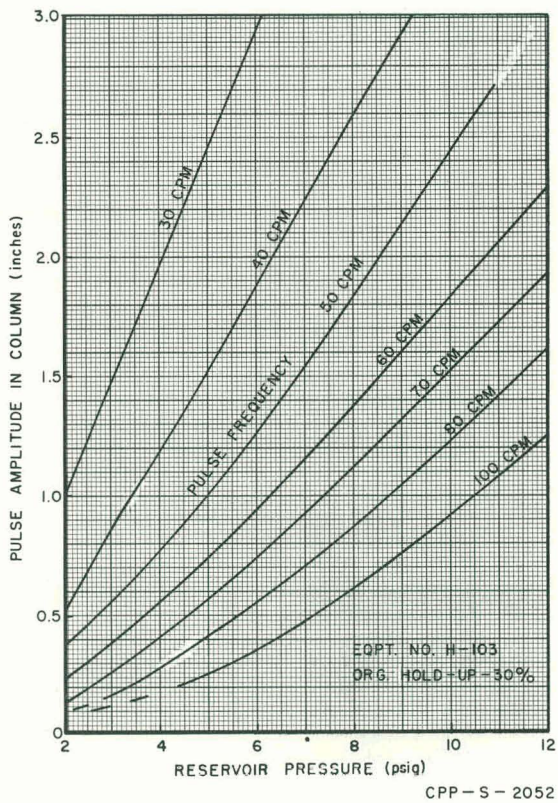

Fig. 13 Operating curves for 1-C column air pulser.

2. EVAPORATOR CONTROL
(E. E. Erickson, Problem Leader, L. A. Jobe)

A study of the dynamics of the new first cycle product evaporator (H-130) system was made in order to check the stability and to estimate the proper controller settings for the system. Although many combinations of transmitter and controller settings may be selected, the recommended settings, based on theoretical calculations from the best information available, are:

Feed flow transmitter-receiver range: 0 to 10 ft/sec.

Steam-flow controller gain: 2.9 (corresponding to 35 percent proportional band).

Density controller gain: 6.9 (corresponding to 14.5 percent proportional band).

This thermosiphon evaporator is to be controlled by a cascade control system. As illustrated in Figure 14, the steam flow to the evaporator is proportioned to the evaporator feed rate by a magnetic flowmeter-controller, whose set point is readjusted by the density controller. The final representation of the evaporator system is that of a well agitated, steam jacketed kettle, as shown in Figure 15. The block diagram for this system is shown in Figure 16. The process blocks consist of two parts: the steady state dimensional gain factor K; and the term defining the transient characteristics (a dimensionless ratio of transformed output to input signal), denoted by G, F, N, or H.

A solute residence time (time constant) of approximately 18 hr justified the change from the original concept of a 20-sec recirculation loop consisting of a heat exchanger process block and five dead times (transport lags). Difficulties were encountered in determining the closed-loop response of the original system, which acted as a regenerative

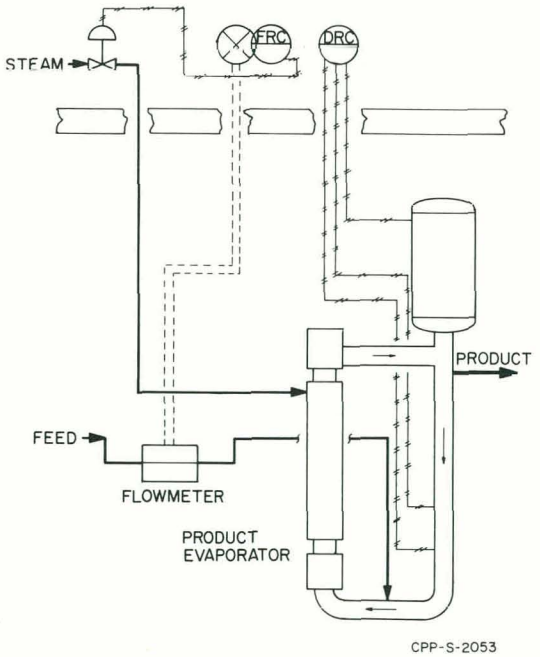

Fig. 14 Thermosiphon evaporator system.

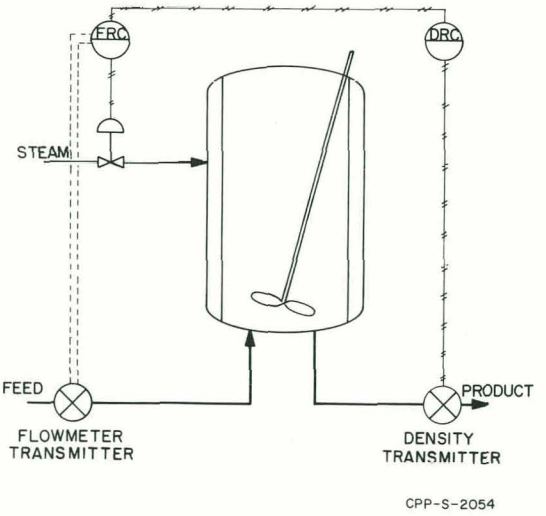

Fig. 15 Modified system concept for H-130 evaporator.

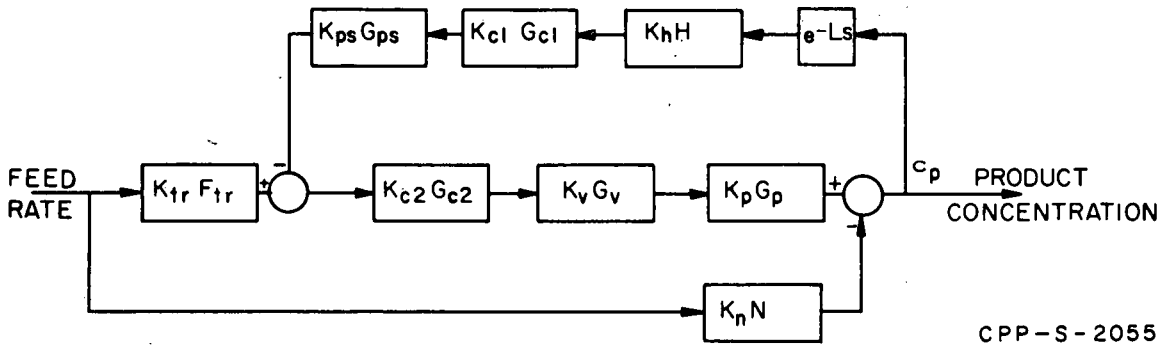

Fig. 16 Block diagram for modified evaporator system.

feed-forward loop. The agitated kettle concept reduced the number of dead times to the single one of sampling.

Since product concentration is the desired variable to be controlled, the uniqueness of the process blocks, K_pG_p and K_nN of Figure 16, is that they must represent, respectively, the concentration effect of steam flow changes and the dilution effect of feed flow changes. The K constants in the process blocks were evaluated by calculating the UNH concentration as a function of percentage increase in feed rate at constant steam flow, or of percentage increase in steam supplied at a constant feed rate. Figure 17 shows the results of

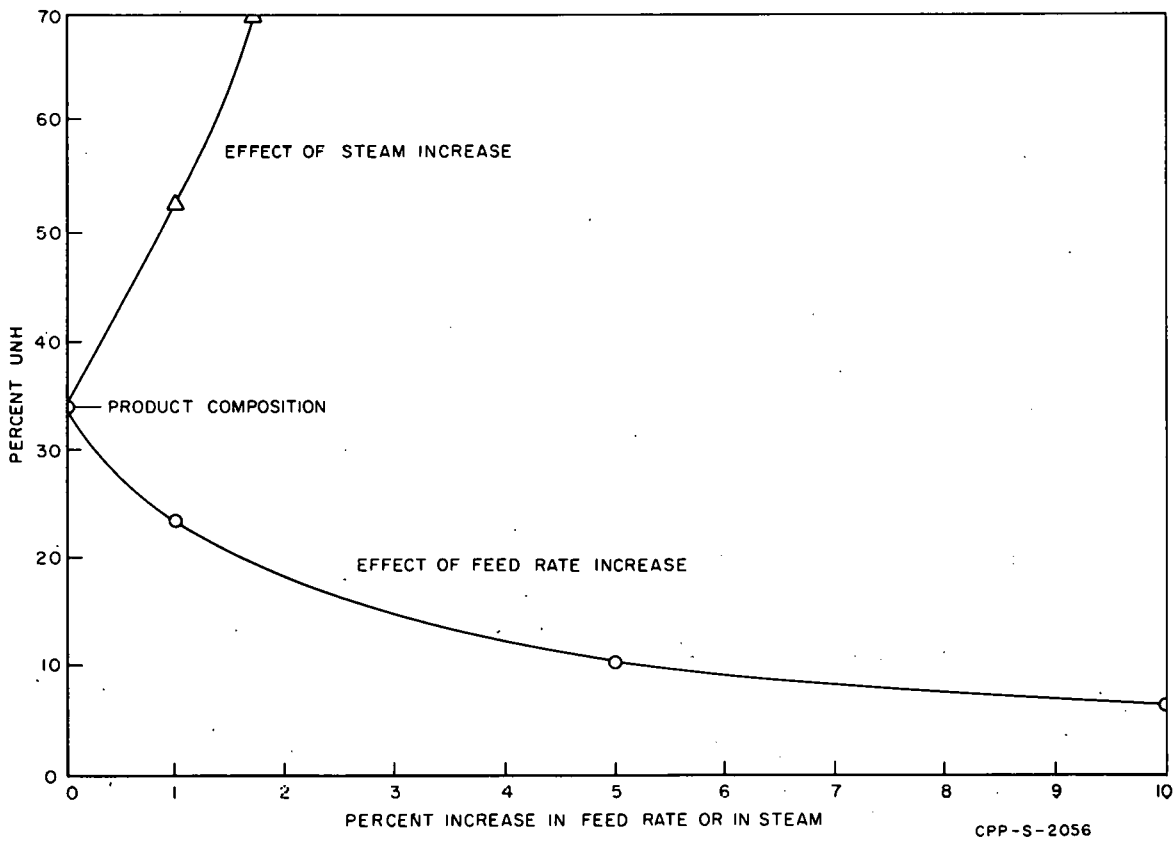

Fig. 17 Effect of increased feed rate at constant steam and of increased steam rate at constant feed upon concentration of UNH.

the calculations. The tangents to the curves at the operating point (corresponding to zero percent change) give the required steady state gain constants, K_p and K_n. The transfer functions of the other blocks are conventional. The values of all transfer functions and steady state gains are given in Table XII.

TABLE XII

VALUES OF STEADY STATE GAINS AND TRANSFER FUNCTIONS

Block	Steady State Gain	Transfer Function	Time Constants
Flow Transmitter	$K_{tr} = 2.33 \times 10^{-3} \frac{mv}{1./hr}$	$F_{tr} = \frac{1}{\tau^2 s^2 + 2\tau_\zeta s + 1}$	$\tau_{tr} = .053$ min
Steam-flow Controller	$K_{c2} = 9.90$ psi/mv	$G_{c2} \simeq 1$	
Steam-valve	$K_v = 98 \frac{lb/hr}{psi}$	$G_v = 1/(\tau_v s + 1)$	$\tau_v = .004$ min
Evaporation Process	$K_p = 4.57 \frac{\%\Delta c}{lb/hr}$	$G_p = 1/(\tau_p s + 1)$	$\tau_p = 1060$ min
Dilution Process	$K_n = 10.32 \frac{\%\Delta c}{1/hr}$	$N \simeq 1$	
Pneumatic Set-Point Adjustment	$K_{ps} \simeq 1$	$G_{ps} \simeq 1$	
Density Measurement	$K_h = \frac{12 \text{ psi}}{33 \%\Delta c}$	$H \simeq 1$	
Density Controller	K_{c1} (to be determined)	$G_{c1} = 1$ (at up to 100 cpm)	

Using the agitated-kettle concept, the transfer functions G_p and N of the process blocks, Figure 16, may be represented by the predominant first-order solute time-constant form: $K/(\tau s + 1)$; where τ is the time constant and s is the Laplacian operator. Effective heat transfer time constants were negligible compared to the solute residence time. For proper control of the system, increased steam flow must compensate for the dilution effect of an increased feed rate. The ratio of recirculation rate to feed rate of approximately 50 will dampen the concentration upset upon a feed rate disturbance. The basic gain of the steam-flow controller was determined by equating the dilution effect through block N to the concentrating effect produced by the product $K_f K_{c2} K_v K_p$. The values of K_f and K_{c2} may be varied, as long as their product remains constant. The K_{c2} value is then used to determine the allowable gain for the density controller within the limits for stability.

3. THE REMOVAL OF TRIBUTYL PHOSPHATE FROM DILUTE AQUEOUS STREAMS

3.1 Design and Testing of a Mixer-Settler for TBP Removal (D. K. MacQueen, Problem Leader; P. Burn, H. V. Chamberlain, E. J. Bailey)

In an effort to improve TBP removal from the strip column product (ICP), and thereby prevent TBP degradation product precipitation in the uranium product evaporator, the diluent scrub column and steam stripper in the continuous aluminum system (CPM) were replaced with a mixer-settler. A five-stage mixer-settler was built and tested in the cold pilot plant. The best apparent TBP removal was down to 3×10^{-3} g/l in the scrubbed ICP. Two additional stages were added to the mixer-settler, and the unit was installed in the CPM system. Later, laboratory data on equilibrium and stripping of TBP showed that an unextractable decomposition product of TBP was causing this apparent lower limit, and that TBP itself should be removed to 4×10^{-4} g/l by the equivalent of two theoretical stages.

3.11 Background. A small amount (~0.07 to 0.2 g/l) of tributyl phosphate (TBP) dissolves in aqueous process streams. If this TBP is not removed from uranium product streams before concentration by evaporation, it decomposes and forms uranyl dibutyl phosphate (UDBP), an extremely insoluble compound, that will plug lines and pumps.

The original CPM head-end extraction system included two pieces of equipment, a scrub column and a steam stripper, for TBP removal from the ICP stream. The scrub column was an unpulsed, organic-continuous, packed column, using a hydrocarbon (Amsco 125-90 W) scrub stream to extract TBP. The scrubbed uranium stream from this column flowed down through a packed steam stripper column to the first cycle product evaporator.

The operation of the CPM equipment train from the ID scrub column to the second cycle feed pumps was never satisfactory. No combination of evaporator feed rate and product concentration would consistently deliver second cycle feed at the design uranium throughput. In addition, there were frequent line plugs and second cycle feed pump failures. At least part of the difficulties were attributed to poor TBP removal, and the replacement of the scrub column and steam stripper was included in the recent CPM system revisions. A review of the design information on which the steam stripper was based indicated that it did not directly apply to the situation at the ICPP, and there was no real reason to believe that the steam stripper would remove TBP to the low levels required. The scrub column design data also left much to be desired, but there was good reason to believe that, with several extraction stages, the required TBP removal could be reached. A mixer-settler was chosen to replace the packed scrub column because the limited head room in the cell would not permit the additional scrub column height needed to increase the number of stages. A mixer-settler also was considered to be a more positive contacting device.

3.12 Design and Testing. A TBP concentration in the feed to the first cycle product evaporator of less than 4×10^{-4} g/l was set as the design objective, based on the evaporator concentration ratio and the available TBP degradation product solubility data. With an estimated equilibrium distribution coefficient of 375, three mixer-settler stages appeared to be adequate. A five-stage mixer-settler box, obtained from KAPL, was available and was used for preliminary tests. This box was under-sized for flowsheet rates (indicated

by excessive entrainment in the product stream), and a larger box was designed and built. The ICPP unit also differed from the KAPL unit by the use of weirs to control interface positions.

The pilot plant tests indicated that five mixer-settler stages would reduce TBP to only 3×10^{-3} g/l in the aqueous product. The accuracy of the analytical procedures that led to this conclusion was questionable. These procedures consisted of a quantitative analysis of the phosphate content of the sample, which was assumed to be from TBP only. The precision of the analysis was rather poor at the phosphate levels represented by TBP contents below 1×10^{-2} g/l. Subsequently, phosphorus-32 was used to make tagged TBP for a series of check runs. The improved accuracy obtained by radioactive counting analyses, however, confirmed the results obtained from chemical analyses.

Two additional stages were added to the ICPP-designed mixer-settler, but it was necessary to release the unit for installation in the plant before pilot plant tests could be made. Subsequent data developed on the physical chemistry of TBP stripping has revealed that the equilibrium distribution coefficient of pure TBP is ~290, down to a concentration as low as 2×10^{-5} g/l, but that an unextractable phosphate species concentrates in the aqueous phase. The phosphorous content of the unextractable species is equivalent to a TBP concentration of 1×10^{-3} g/l; consequently, the analytical procedures cannot detect TBP removal below this limit. Kinetic experiments indicated the residence time in each mixer stage was too short, and a maximum of about 60 percent removal per stage would be expected in the box as designed. In view of these facts, which were not available at the time the plant mixer-settler was designed, a more simple, two- or three-stage box could now be built to remove TBP below 4×10^{-4} g/l; however, the unextractable phosphates would remain. No effective means of removing these residual phosphate compounds has yet been found.

3.2 Laboratory Studies on the Removal of Tributyl Phosphate from Aqueous Streams (H. T. Hahn, Problem Leader; E. M. Vander Wall, D. L. Bauer)

The laboratory work reported in this quarter concerns, first, the preparation of a relatively large amount of labelled TBP. Use of this TBP in the pilot plant demonstrated that the five-stage mixer-settler unit reduced the apparent residual TBP content to a value no better than 2.7×10^{-3} g/l. Succeeding work has involved a study of the physical chemistry of the TBP-Amsco-water system and a determination of the reasons for the failure of the mixer-settler unit to meet the design specifications.

3.21 Materials and Analyses. The activated TBP was prepared from irradiated P_2O_5, via silver orthophosphates [14].

The product was purified by vacuum distillation, and the fraction boiling between 122 and 124°C at two mm Hg was used in this work. The specific activity of the product was initially of the order of 30 millicuries/ml.

Aqueous solutions of TBP were prepared by weighing the TBP into known volumes of solution. These solutions were then shaken for several hours to insure complete dissolution of the TBP. The organic solutions of TBP were prepared in an analogous manner, but no extensive agitation was required. Amsco 125-90 W was used as the organic phase in these studies.

The TBP distribution coefficients were obtained by shaking portions of stock solutions with the desired organic or aqueous phase in separatory funnels. Active samples were analyzed for phosphate by counting techniques. The average material balance with standard deviation was 104.1 ± 12.6 percent for the samples analyzed in this manner. In experiments in which no TBP tracer was used, analysis for total phosphate was by a colorimetric method. Only the higher phosphate concentrations could be analyzed by this method.

3.22 Kinetics of TBP Extraction Between Amsco and Water. To determine the mixing time required to attain equilibrium in this system, experiments were performed in which samples were removed from the separatory funnel at ten sec intervals. The aqueous-to-organic volume ratio was 10:1. The TBP was spiked into distilled water and shaken with Amsco. The data obtained for various mixing periods are presented in Curve A of Figure 18. The settling periods varied from 15 to 30 sec; two samples shaken 10 sec and allowed to settle 15 sec contained $(2.19 \pm 0.02) \times 10^{-2}$ g TBP/l of H_2O, while four other samples shaken 10 sec and allowed to settle for 60 sec contained $(2.19 \pm 0.52) \times 10^{-2}$ g TBP/l of H_2O. Therefore, the variations encountered in settling time during these experiments are not significant.

Stripping is approximately 78 percent complete after 10 sec, 94 percent complete after 15 sec, and 97.5 percent complete after 30 sec of shaking. The system appears to reach equilibrium within two min. Since pilot plant operating lines obtained from the mixer-settler indicated 50 to 60 percent efficiency per stage, longer residence times were recommended. Further gains also may be made in mixer performance since laboratory efficiencies of 50 to 60 percent were achieved in roughly nine sec vs an estimated 18 sec residence in the pilot plant runs.

Experiments with TBP in an aqueous solution of 0.1N HNO_3 and 1.28 g U/l showed no significant TBP concentration differences as the shaking time ranged from two min to 67 hr, with a five-min settling time. To establish this settling time as adequate, an aqueous solution was sampled after five min and after 88 hr. There was no significant difference in the TBP concentration of these samples.

The time required to attain equilibrium during the transfer of TBP from Amsco to distilled water also was investigated. In this instance, the settling times also ranged from 15 to 30 sec. The data obtained are presented in Curve B of Figure 18. Again it is apparent that equilibrium is reached within a two-min period.

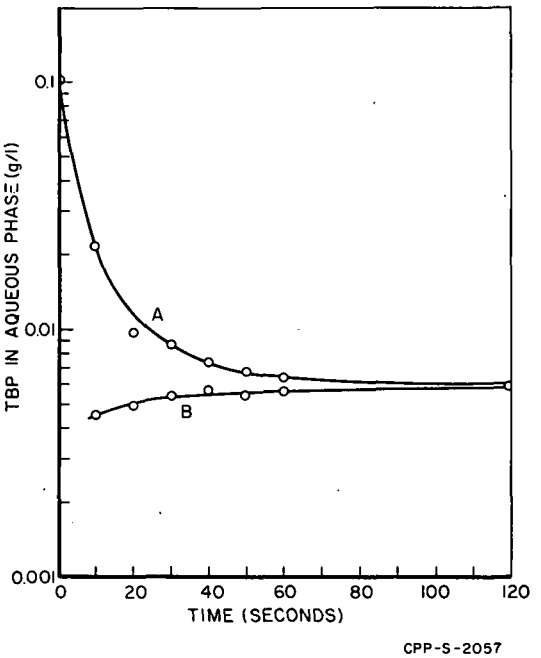

Fig. 18 Mixing time required to reach equilibrium in TBP distribution between Amsco and distilled water. A. Starting with TBP in water; B. Starting with TBP in Amsco.

3.23 TBP Distribution Between Amsco and Water

Determination of the Equilibrium Line. According to the kinetic data, equilibrium was attained in this system within a two-min mixing period; therefore, the phases were shaken for two min and then allowed to settle for five min before samples were withdrawn. The aqueous-to-organic volume ratios ranged from 64:1 to 10:1; most of the experiments were performed at a 10:1 ratio. The distribution coefficients obtained from the various phase ratios were not significantly different; this insures that the system was at equilibrium. The data used to determine the equilibrium line were all single stage contacts.

These data were compiled from five types of experiments. First, the Amsco was spiked with radioactive TBP and then contacted with an aqueous phase which contained 0.1N HNO_3 and 1.28 g uranium/l. Second, Amsco was spiked with radioactive TBP and then contacted with water. Third, the aqueous phase (0.1N HNO_3 and 1.28 g U/l) was spiked with radioactive TBP before being contacted with Amsco. Fourth, radioactive TBP was dissolved in water which was then contacted with Amsco. Fifth, unirradiated TBP was dissolved in distilled water and contacted with Amsco.

The aqueous-spiked TBP solutions were found to contain a phosphate species which remained preferentially in the aqueous phase. The concentration of TBP in the aqueous phase therefore required a correction factor to obtain a valid value for the equilibrium curve. After this correction was made, there appeared to be no significant difference in the TBP distribution coefficient derived from the five different types of experiments. This indicates that 0.1N HNO_3 and 1.28 g uranium/l have a negligible effect on the equilibrium system.

The average value, with its standard deviation for the TBP distribution coefficient between Amsco and the aqueous phases described, was 290 $\pm$ 31. The data are presented as the linear plot in Figure 19. The TBP concentration in the aqueous phases ranged from 3×10^{-5} to 3×10^{-2} g/l.

3.24 Deviations from the Equilibrium Line

Presence of species other than TBP which contain P-32. Multistage contacting of the phases, where the aqueous phase contained the TBP tracer, produced TBP distribution curves which turned down from the original equilibrium line. An example of this tailing off is a solution of 0.1N HNO_3 containing 1.28 g U/l and 77.2 mg TBP/l which had four separate contacts with fresh Amsco. The data obtained are presented as Curve 2 in Figure 19.

To confirm that the system was at equilibrium, similar solutions were shaken continuously for periods up to three days with no appreciable concentration changes occurring. Therefore, either another phosphate species is present or some reagent impurity causes the digression from the equilibrium line. Reagent impurities (excluding phosphorous compounds) were dismissed as a factor, when the same digression occurred in a system containing only Amsco, distilled water and the TBP stock. This foreign species preferred the aqueous phase to such an extent that often after four contact stages the aqueous phase contained more phosphorous 32 than the organic phase.

As further evidence for the validity of the TBP equilibrium line established by single contacts, an experiment was performed in which the distilled-water

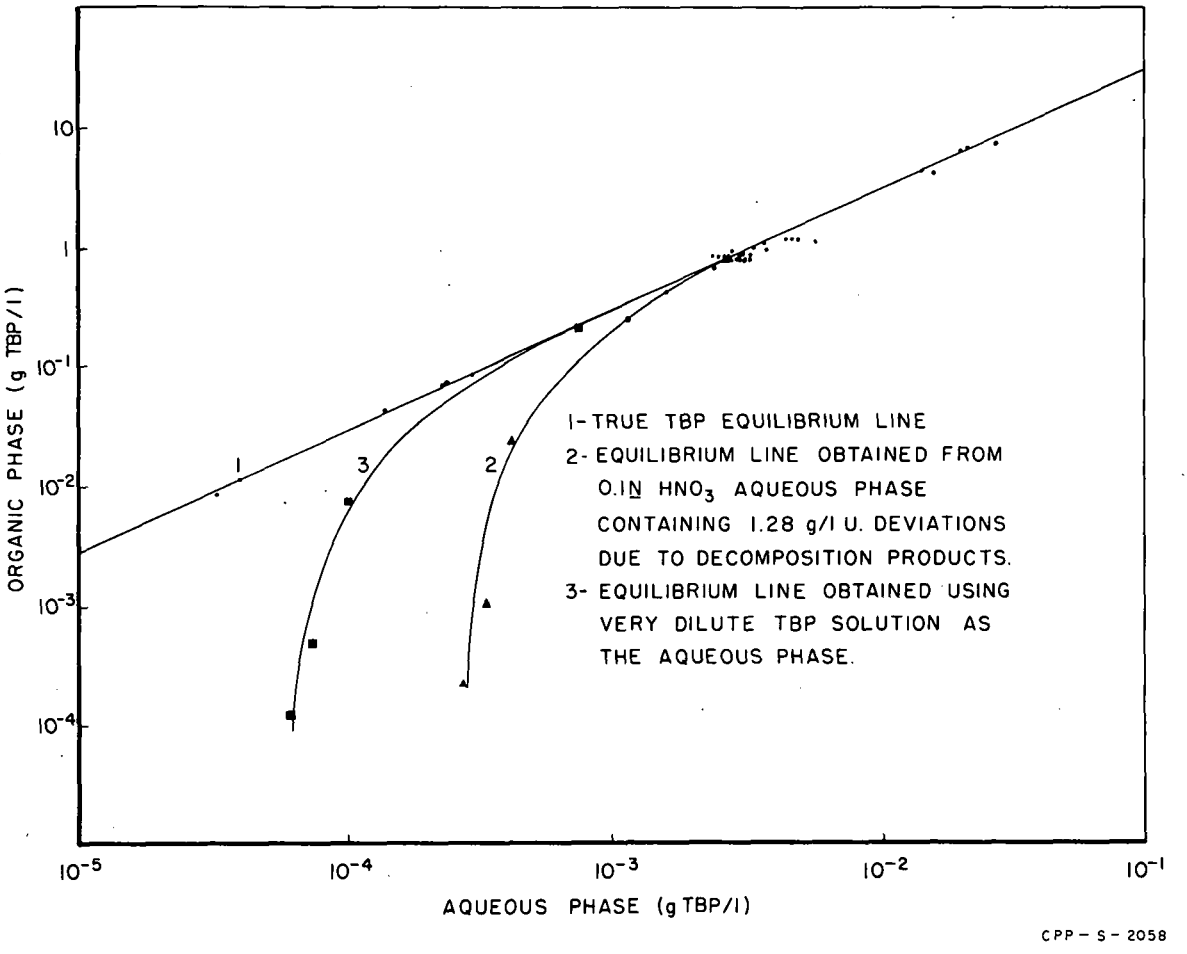

Fig. 19 TBP distribution between Amsco and water.

phase was spiked by contact with an Amsco-radioactive TBP solution. The resulting aqueous phase was then contacted with fresh Amsco three times. The data obtained are presented in Curve 3 of Figure 19. Since dilution should not affect the equilibrium line, this curve establishes that Curve 2 - Figure 19 is not a true TBP equilibrium representation, and that it is indeed another species of phosphate which causes the deviation from the true equilibrium line.

Since the radiation present in these solutions is at least partially responsible for TBP decomposition, a series of experiments was conducted in which non-radioactive TBP (vacuum distilled from CaO) was dissolved in the aqueous phase and contacted with Amsco in four stages in order to determine whether hydrolysis also was involved. The first stage concentrations always coincided with the equilibrium line. Unfortunately, after the first contact stage in each case, the concentration of TBP in the aqueous product was already below the limits of the colorimetric method of analysis. Therefore, the cause of TBP decomposition is not unequivocally established.

3.25 Rate of TBP Decomposition into Other Species Containing Phosphorous-32 The concentration of the aqueous-preferring phosphate species was found to increase with time. An analysis of the data obtained over a period of 24 days

shows that the TBP decomposition can be represented by a first order rate law. The rate constant for this decomposition is about 1×10^{-3}/day. This decomposition appears to occur with the same rate constant whether the TBP exists as a dilute solution in distilled water or whether it is the distilled stock. This fact implies either that water may still be present in the distilled TBP to cause hydrolysis, or that radiolysis in the organic phase balances hydrolysis in the aqueous phase.

In the 0.1N HNO_3 solutions which contain 1.28 g uranium/l. the decomposition rate of TBP is greatly accelerated as compared to TBP in water. The decomposition rate still appears to be first order and the rate constant is approximately 4×10^{-2}/day. The increased decomposition rate probably is due to a photochemical reaction which can occur in the presence of uranium. No attempt was made to exclude these stock solutions from light.

4. ELECTRICAL CONDUCTANCES IN THE ACETIC ACID-HEXONE-WATER AND NITRIC ACID-HEXONE-WATER SYSTEM

(H. T. Hahn, Problem Leader; D. P. Pearson)

A planned study of extraction column kinetics will require a method for continuous monitoring of the extracted species at selected points in the column. It has been deemed desirable to follow this concentration in both phases to permit calculation of material balances.

The use of electrical conductance was proposed as one method of analysis. Since considerable extraction data were available for the acetic acid-hexone-water system and the equilibrium relationship was reasonably linear, this system was investigated first. Other work reported this quarter concerns conductance measurements of the nitric acid-hexone-water system.

The conductances were measured at 25°C, and acid concentrations were determined by titration. The results for the acetic acid-hexone-water system are shown in Figure 20.

In order to use conductance as a means of following changes in acid concentration and the approach to a steady state, the conductance must change significantly with acid concentration. This is not true for acetic acid in hexone below 0.2M (aqueous) or for acetic acid in water above 1M. Between these two concentrations, both phases could be monitored successfully for acetic acid; however, the useful range is relatively narrow.

Both phases could be monitored over a considerably wider concentration range if nitric acid were used. The results of conductance and concentration measurements for the nitric acid-hexone-water system are shown in Figure 21. A disadvantage of nitric acid is that the extraction coefficient ($E°_a$) is about 0.05, compared with 0.5 for acetic acid. This means that changes in aqueous nitric acid concentration will be relatively small compared to organic phase changes, and hence less sensitivity is available for aqueous phase analysis.

If, in the development of equipment, it is found impractical to monitor both phases, the analytical situation actually would be considerably simplified,

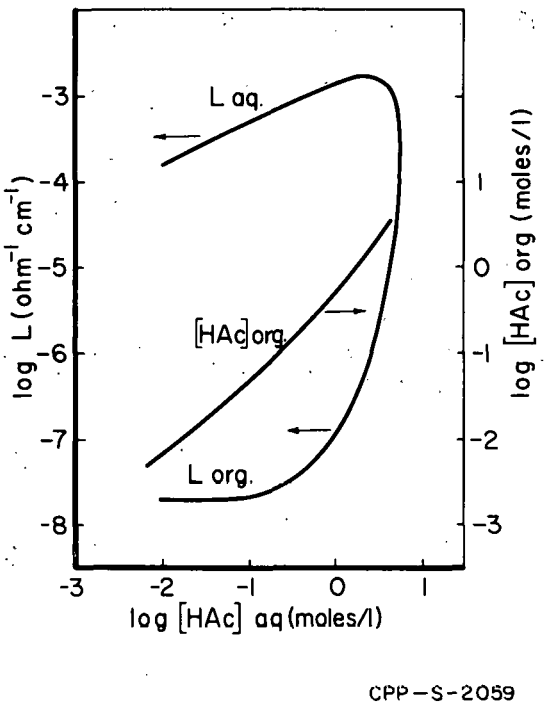

Fig. 20 Equilibrium acid concentrations and electrical conductances in the system acetic acid - hexone - water at 25°C.

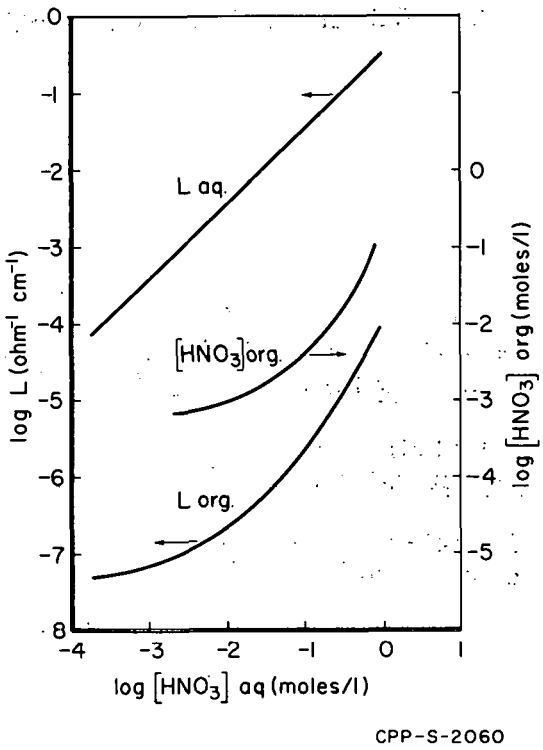

Fig. 21 Equilibrium acid concentrations and electrical conductances in the system nitric acid - hexone - water at 25°C.

since either acid-phase combination, alone, offers at least a tenfold concentration range in which the conductance is a sensitive function of acid concentration.

It has been observed that the mutual solubilities of water and hexone vary with acid concentrations. Measurement of the effect of this variation on the conductances of the phases is planned, since during column operation the mutual solubility will be somewhere between the solubility under initial conditions and the equilibrium solubility.

VII. REPORTS AND PUBLICATIONS ISSUED DURING THE QUARTER

1. IDO REPORTS ISSUED

IDO-14559, Interim Report on the Development of an Air Pulser for Pulse Column Application, by M. E. Weech, R.S. P'Pool and D. K. MacQueen

IDO-14561, Air Lift Performance at Low Liquid Rates Using Over-Size Piping and Lateral Runs, by H. V. Chamberlain

IDO-14562, Mixing and Evaporation in a Packed Vessel, by G. K. Cederberg and J. A. Buckham

VIII. REFERENCES

1. J. R. Bower, Ed., Chemical Processing Technology Quarterly Progress Report, IDO-14560, (January - March 1961).
2. E. M. Vander Wall and E. M. Whitener, "Concentrated Nitric and Dilute Hydrofluoric Acid Mixtures in Dissolution of Zirconium Metal", Ind. Eng. Chem. V, 51, No. 1, p. 51-54, (January 1959).
3. J. R. Bower, Ed., Chemical Processing Technology Quarterly Progress Report, IDO-14534, p. 60-62, (April - June 1960).
4. O. W. Parrett, Modifications for the STR Fuel Recovery Process , IDO-14522, (December 1960).
5. T. A. Gens and W. E. Clark, Laboratory Development of the Perflex Process for Dissolution of Uranium Alloy Fuels in Hydrofluoric Acid - Hydrogen Peroxide Solutions , CF 59-11-23, (November 1959).
6. H. W. Miller, Phase Studies of Aqueous Solutions of Uranyl Nitrate and Ammonium Hydroxide , IDO-14313, (September 1954).
7. Redox Technical Manual, HW-18700 (Book I of III), Fig. IV-17, (July 1951), (Rpt: Secret-RD).
8. O. W. Parrett, The Determination of Excessive Emulsification by Coalescence Behavior Measurements , IDO-14486, (November 1954).
9. G. A. Huff, I. L. Daggett, R. D. Fletcher and M. E. Jacobson, Remote Dissolution and Analytical Program for Irradiated Thorium , IDO-14557, (July 1961).
10. J. R. Bower, Ed., Chemical Processing Technology Quarterly Progress Report, IDO-14567, (April - June 1961).
11. K. R. Holtzinger, et al, "A Polarographic Method for Determining the Total Cation Exchange Capacity of Soils", Soil Science, 77: p. 137-142, (1954).
12. J. R. Bower, Ed., Chemical Processing Technology Quarterly Progress Report, IDO-14553, (October - December 1960).
13. M. E. Weech, R. S. P'Pool and D. K. MacQueen, Interim Report on the Development of an Air Pulser for Pulse Column Application , IDO-14559, (September 1961).
14. W. E. Baldwin and C. E. Higgins, The Preparation of Tri-n-Butyl Phosphate , ORNL-887, p. 32, (February 1951).

PHILLIPS
PETROLEUM
COMPANY

ATOMIC ENERGY DIVISION